Question

147 筋ジストロフィー患者が来院したら？

Answer

日常歯科診療では口腔ケアの指導が重要である。病型によって，顎関節拘縮による開口制限や習慣性顎関節脱臼が生じやすいため，処置での開口に注意を要する。治療による呼吸抑制や不整脈惹起，全身麻酔による悪性高熱に注意を要する。

解説　筋ジストロフィーは「筋線維の壊死・変性を主病変とし，臨床的には進行性の筋力低下と筋萎縮をみる，遺伝性疾患」と定義される。小児ではデュシェンヌ型筋ジストロフィー（Duchenne muscular dystrophy：DMD），成人では筋強直性ジストロフィー（myotonic dystrophy：MyD）が多い[1]。

筋ジストロフィーでは開咬や反対咬合といった不正咬合，歯列不正がみられることが多い。DMDでは巨舌が，MyDでは斧様顔貌が影響する[2]。嚥下障害はMyDでほぼ必発であるが，嚥下機能が比較的保たれるDMDでも，輪状咽頭筋弛緩不全による通過障害，咽喉頭筋力低下，脊柱側弯による頸部変形のため嚥下障害を来す。筋ジストロフィーでは呼吸不全のため肺炎を生じやすい。以上の観点から，筋ジストロフィーの日常歯科診療では口腔ケアの指導が重要である。上肢麻痺のため口腔ケアを介助に依存する患者では，介助者への指導を要する。MyDはこだわりが強い反面，自分がこだわらないことには関心がない心理的特徴があり，口腔ケア指導に根気を要する。

DMDでは顎関節拘縮による開口制限と巨舌のため，口腔内での視野確保が困難なことがある。MyDでは咬筋をはじめ顔面筋の萎縮が強く，習慣性顎関節脱臼を来すことがある。いずれにしても，歯科的処置における無理な開口は避けるべきである。また，嚥下障害があることから，処置中の唾液貯留に特に注意を払い，気道閉塞を避けるための体位の工夫や頻繁な吸引が求められる。

筋ジストロフィー患者は，唾液による気道閉塞をはじめ呼吸状態が処置中に悪化することがある。特に鼻マスク式人工呼吸に常時依存する患者の歯科処置には慎重を要する。心不全を来した患者はアドレナリン（エピネフリン）で不整脈や動悸が生じることがある[3]。筋ジストロフィーは全身麻酔で悪性高熱が生じる危険が高いとされ，準備と配慮を要する。

（尾方　克久）

Column

筋ジストロフィー診療の新たな課題と歯科診療

呼吸不全に対する人工呼吸療法と気道クリアランス技術の発達，心不全薬物療法の進歩により，筋ジストロフィーの生命予後は改善している。かつて18歳前後であったDMDの平均死亡年齢は，現在では約30歳になった。しかしこれらは，筋ジストロフィーの本質的病態を抑止するものではないので，予後改善に伴い新たな臨床的問題に直面している。進行期DMDでの咀嚼嚥下障害，鼻マスク式人工呼吸の口からの気流漏れによる換気効率低下など，歯科診療が必要な課題は多い。また患者にとって“食”と“味”は大きな楽しみである。「どれだけ生きるか」を目指す時代から「どう生きるか」を見据えるようになった現代の筋ジストロフィー診療において，歯科診療の重要性は一層高まっている。

Reference
1）尾方克久：筋ジストロフィー．Clin Neurosci 27(8)：913-916, 2009
2）佐々木俊明：筋ジストロフィーの歯科学的特徴．医療61(12)：786-790, 2007
3）松村　剛：筋ジストロフィーの臨床現場における歯科学的問題．医療61(12)：781-785, 2007

Journal of the Neurological Sciences 309 (2011) 9–11

Contents lists available at ScienceDirect

Journal of the Neurological Sciences

journal homepage: www.elsevier.com/locate/jns

A novel mutation in the calcium channel gene in a family with hypokalemic periodic paralysis

Makito Hirano [a], Yosuke Kokunai [b], Asami Nagai [c], Yusaku Nakamura [a], Kazumasa Saigoh [d], Susumu Kusunoki [d], Masanori P. Takahashi [b,*]

[a] Department of Neurology, Sakai Hospital Kinki University Faculty of Medicine, Sakai, Osaka, Japan
[b] Department of Neurology, Osaka University Graduate School of Medicine, Suita, Osaka, Japan
[c] Department of Internal Medicine, Tohokashiba Hospital, Japan
[d] Department of Neurology, Kinki University, Faculty of Medicine, Osakasayama, Osaka, Japan

ARTICLE INFO

Article history:
Received 10 June 2011
Received in revised form 23 July 2011
Accepted 26 July 2011
Available online 19 August 2011

Keywords:
Hypokalemic periodic paralysis
Hyperkalemia
Calcium channel
Voltage sensor
Diagnostic difficulty
Increased CK

ABSTRACT

Hypokalemic periodic paralysis (HypoPP) type 1 is an autosomal dominant disease caused by mutations in the Ca(V)1.1 calcium channel encoded by the *CACNA1S* gene. Only seven mutations have been found since the discovery of the causative gene in 1994. We describe a patient with HypoPP who had a high serum potassium concentration after recovery from a recent paralysis, which complicated the correct diagnosis. This patient and other affected family members had a novel mutation, p.Arg900Gly, in the *CACNA1S* gene.

1. Introduction

Hypokalemic periodic paralysis (HypoPP) is an autosomal dominant disease caused by mutations in either the Ca(V)1.1 calcium channel encoded by the *CACNA1S* gene (HypoPP type 1) or the Na(V)1.4 sodium channel encoded by the *SCN4A* gene (HypoPP type 2) [1]. HypoPP type 1 is more common than HypoPP type 2 (1:5–8). In HypoPP type 1, only seven mutations have been found since the discovery of the causative gene in 1994 [2]. However, the prevalence of HypoPP is not extremely low (1:100,000), suggesting that a few common mutations affect many families [3]. The Ca(V)1.1 channel consists of four domains, and each domain has S1 to S6 transmembrane segments. All mutations but one rare one (p.Val876Glu) [4] are involved in arginine residues in the S4 segments of the calcium channel [2,3,5–7]. A recent study proposed a gating pore cation leak current caused by loss of a positive charge of arginine in S4 voltage sensors as a common pathomechanism of HypoPP [1,8].

We describe a patient with HypoPP who had a high serum potassium concentration after recovery from paralysis, which complicated the correct diagnosis. This patient had a novel mutation, p.Arg900Gly, in the *CACNA1S* gene.

2. Patients

The proband (patient 1) was a 41-year-old man who started to have periodic episodes of paralysis, occurring about five times a year, since the age of 21 years. Each episode lasted 12 hours to 2 days. Hard physical exercise seemed to induce paralysis and was therefore avoided. Overeating, but not coldness, also induced paralysis. On a careful, detailed interview, he recalled that he had had a history of hypokalemia at the time of the previous episode of paralysis, but the value was not currently available since the clinic he had visited had permanently closed. He also reported having received potassium supplements at that time, which seemed effective, but were soon discontinued for no apparent reason. A family tree (Fig. 1A) suggested a pattern of autosomal dominant inheritance (Fig. 1A). Two days after a recent episode of paralysis he visited our clinic. Muscle strength was normal, with no muscular atrophy. Laboratory tests showed increased levels of potassium (5.4 mEq/l, normal 3.3–5.0 mEq/l), CK (3233 IU/ml, normal 45–190 IU/ml), AST (104 IU/l, normal 10–40 IU/ml), and ALT (54 IU/ml, normal 5–45 IU/ml). Blood sugar was only slightly decreased to 69 mg/dl (normal 70–139 mg/dl). Other data, including thyroid function, were normal: Na 144 mEq/l, Cl 104 mEq/l, TSH 0.89 mU/ml (normal 0.34–3.88), fT3 3.8 pg/ml (normal 2.1–4.1 pg/ml), and fT4 1.5 ng/ml (normal 1.0–1.7 ng/ml). Electrocardiography and chest radiography showed normal findings. Electromyography showed no myotonic discharges or myogenic changes during non-

* Corresponding author at: Department of Neurology Osaka University Graduate School of Medicine, 2-2 Yamadaoka, Suita 565-0871, Osaka, Japan.
E-mail address: mtakahas@neurol.med.osaka-u.ac.jp (M.P. Takahashi).

0022-510X/$ – see front matter © 2011 Elsevier B.V. All rights reserved.
doi:10.1016/j.jns.2011.07.046

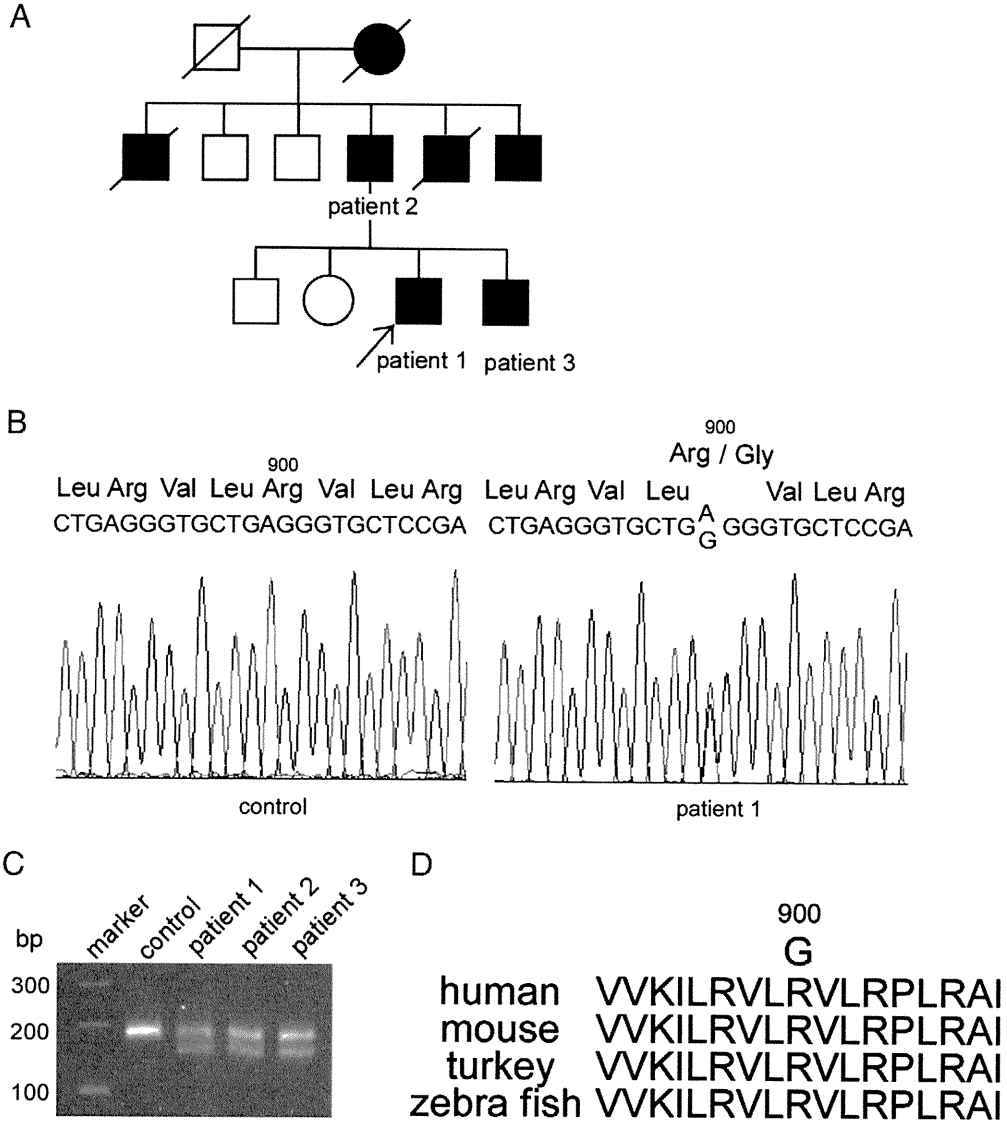

Fig. 1. (A) A family tree of the patient 1 (arrow). This family tree suggests an autosomal dominant pattern of inheritance. (B) The patient had a heterozygous A-to-G transition, resulting in the substitution of Arg by Gly at the 900 residue. (C) PCR-restriction fragment length analyses with a mismatch primer confirmed that Patients 1–3 were heterozygous for the p.Arg900Gly mutation. (D) The Arg at the 900 position is phylogenetically conserved.

paralytic periods. After 19 days, all abnormal blood test values had normalized.

Patient 2 (69 years), the father of the proband, had paralytic attacks since the age of 13 years. Most attacks, occurring 5 times/year, were mild or partial, but severe episodes occurred 10 times over the course of 37 years. Paralysis was induced by hard physical exercise and overeating, but not coldness. He had not been examined in any medical institutions during paralysis. He has had no attacks since the age of 50 years. Patient 3 (35 years), a younger brother of the proband, started to have mild paralytic attacks since the age of 13 years and severe ones since age 15. He also recalled that he had had a history of hypokalemia during paralysis, but the value was not currently available. Recently, he had severe attacks 10 times/year, induced by hard exercise and overeating, but not by coldness.

After obtaining written informed consent from Patient 1, a genetic analysis was performed as described previously [2,3,5]. Patients 2 and 3 agreed to genetic testing, but the mother of the proband declined. A novel heterozygous A-to-G transition was identified in the *CACNA1S* gene (c.2698A>G), resulting in a missense change (p.Arg900Gly, Fig. 1B). This mutation was confirmed by PCR-restriction fragment length analyses as follows. The forward primer carried two nucleotide substitutions (ex21mF: 5′-GTGCCATCTCCGTGGTGAAGAcCaT-GAGGGTGCT-3′, lower case letters mean substituted nucleotides) to create the endonuclease *Xcm*I (CCANNNNNNNNTGG) site in a PCR fragment only from a mutant allele. The reverse primer was 5′-GGTCCCAGCCATGGCTGGGCTGA-3′. The PCR-amplified mutant fragment (179 bp) was digested into two fragments (29 and 150 bp), though only the larger fragment was visible. The normal fragment remained undigested. This mutation was present in Patients 1–3, but not in 100 control chromosomes (Fig. 1C). This Arg900 residue is highly conserved among humans, mice, turkeys, and zebra fish (Fig. 1D).

3. Discussion

We found a novel mutation in a patient with HypoPP type 1. This mutation in the S4 segment of the domain III affects the same residue as the previously identified mutation p.Arg900Ser [3]. Similar to previous other mutations involving arginine residues, the positive charge of arginine was abolished by a neutral amino acid, glycine. The Arg900 residue is phylogenetically conserved. Thus, this novel

p.Arg900Gly mutation may cause a gating pore current leak and is most likely causative for HypoPP.

Our patient had a high serum potassium concentration at the visit to our clinic after recovery from paralysis, which complicated the correct diagnosis. However, such hyperkalemia during recovery periods in HypoPP has been described previously, although mutations in either the calcium channel or sodium channel were not specified [9]. To our knowledge, mutations in the *CACNA1S* gene have not previously been associated with hyperkalemic periodic paralysis. Consistent with this, our patient presented with previous episodes of hypokalemia. Although hyperkalemia might have simply been a rebound response to hypokalemia, another possible explanation is that hypokalemia during paralysis may have destabilized muscular membranes, releasing intramuscular potassium into serum. This hypothesis may be supported by the temporal elevation of CK in our patient.

A previous study reported at least one patient with p.Arg900Ser mutation, a mutation occurring in the same residue as ours. The patient had a typical HypoPP phenotype, although detailed clinical information was not provided [3]. Attacks began to occur in the second decade and were associated with low potassium levels or with provocative factors that reduced serum potassium levels. In our patients, disease developed at 13 to 21 years of age and was accompanied by typical HypoPP episodes. Thus, mutations involving the Arg900 residue seem to be associated with a typical phenotype.

In summary, we found a novel mutation in the *CACNA1S* gene, which further supports the gating pore current hypothesis as a pathomechanism of HypoPP. Because this is only the eighth mutation identified over the course of 17 years, further discovery of mutations may provide further insight into voltage-gated channels as well as the pathomechanism of HypoPP.

Acknowledgments

This study was supported partly by Research Grants for Intractable Disease from the Ministry of Health, Labour and Welfare (to MPT).

References

[1] Cannon SC. Voltage-sensor mutations in channelopathies of skeletal muscle. J Physiol 2010;588(Pt 11):1887–95.
[2] Ptacek LJ, Tawil R, Griggs RC, Engel AG, Layzer RB, Kwiecinski H, et al. Dihydropyridine receptor mutations cause hypokalemic periodic paralysis. Cell 1994;77(6):863–8.
[3] Matthews E, Labrum R, Sweeney MG, Sud R, Haworth A, Chinnery PF, et al. Voltage sensor charge loss accounts for most cases of hypokalemic periodic paralysis. Neurology 2009;72(18):1544–7.
[4] Ke T, Gomez CR, Mateus HE, Castano JA, Wang QK. Novel CACNA1S mutation causes autosomal dominant hypokalemic periodic paralysis in a South American family. J Hum Genet 2009;54(11):660–4.
[5] Jurkat-Rott K, Lehmann-Horn F, Elbaz A, Heine R, Gregg RG, Hogan K, et al. A calcium channel mutation causing hypokalemic periodic paralysis. Hum Mol Genet 1994;3(8):1415–9.
[6] Elbaz A, Vale-Santos J, Jurkat-Rott K, Lapie P, Ophoff RA, Bady B, et al. Hypokalemic periodic paralysis and the dihydropyridine receptor (CACNL1A3): genotype/phenotype correlations for two predominant mutations and evidence for the absence of a founder effect in 16 caucasian families. Am J Hum Genet 1995;56(2):374–80.
[7] Chabrier S, Monnier N, Lunardi J. Early onset of hypokalaemic periodic paralysis caused by a novel mutation of the CACNA1S gene. J Med Genet 2008;45(10):686–8.
[8] Sokolov S, Scheuer T, Catterall WA. Gating pore current in an inherited ion channelopathy. Nature 2007;446(7131):76–8.
[9] Lehmann-Horn F, Rudel R, Jurkat-Rott K. Nondystrophic myotonias and periodic paralyses. In: Engel AG, editor. Myology. McGraw Hill Medical Publishing Division; 2003.

Misregulation of miR-1 processing is associated with heart defects in myotonic dystrophy

Frédérique Rau[1–4], Fernande Freyermuth[1–4], Charlotte Fugier[1–4], Jean-Philippe Villemin[5], Marie-Christine Fischer[1–4], Bernard Jost[1–4], Doulaye Dembele[1–4], Geneviève Gourdon[6–8], Annie Nicole[6–8], Denis Duboc[8,9], Karim Wahbi[10–13], John W Day[14], Harutoshi Fujimura[15], Masanori P Takahashi[16], Didier Auboeuf[10], Natacha Dreumont[1–4], Denis Furling[10–13] & Nicolas Charlet-Berguerand[1–4]

Myotonic dystrophy is an RNA gain-of-function disease caused by expanded CUG or CCUG repeats, which sequester the RNA binding protein MBNL1. Here we describe a newly discovered function for MBNL1 as a regulator of pre-miR-1 biogenesis and find that miR-1 processing is altered in heart samples from people with myotonic dystrophy. MBNL1 binds to a UGC motif located within the loop of pre-miR-1 and competes for the binding of LIN28, which promotes pre-miR-1 uridylation by ZCCHC11 (TUT4) and blocks Dicer processing. As a consequence of miR-1 loss, expression of GJA1 (connexin 43) and CACNA1C (Cav1.2), which are targets of miR-1, is increased in both DM1- and DM2-affected hearts. CACNA1C and GJA1 encode the main calcium- and gap-junction channels in heart, respectively, and we propose that their misregulation may contribute to the cardiac dysfunctions observed in affected persons.

Myotonic dystrophy, which is the most common muscular dystrophy in adults, is characterized by multiple symptoms that include muscle weakness, myotonia, cardiac defects, cataracts, insulin resistance and neuropsychiatric impairment. Myotonic dystrophy type 1 (DM1) is caused by an expansion of CTG repeats located within the 3′ noncoding region of the *DMPK* gene[1–3], whereas myotonic dystrophy type 2 (DM2) is caused by an expansion of CCTG repeats located within the first intron of the *ZNF9* (also known as *CNBP*) gene[4]. The mutant RNA, which contains 100 to several thousand CUG or CCUG repeats, is retained in nuclear aggregates that sequester the MBNL1 RNA binding protein[5–8]. Furthermore, the expression of CUGBP1(also known as *CELF1*) is increased in some tissues of DM1-affected people[9,10]. MBNL1 and CUGBP1 are splicing regulators, and their alterations in people with myotonic dystrophy result in misregulation of the alternative splicing of several pre-mRNAs[11–13], including those encoded by the muscle chloride channel gene *CLCN1* and the insulin receptor gene *INSR*, resulting in myotonia and insulin resistance, respectively[14–17]. However, the molecular mechanisms underlying the cardiac defects, which affect 80% of people with DM1 and DM2 and represent the second most common cause of their death, are unclear. Cardiac involvements in affected persons[18–21] and in mouse models[22,23] are characterized by nonspecific changes such as interstitial fibrosis and fatty infiltration, which lead to degeneration of the conduction system and to fatal atrioventricular blocks. Furthermore, people with myotonic dystrophy are also characterized by atrial and ventricular tachyarrythmias of unknown causes, which may explain the occurrences of sudden cardiac death observed in these people despite pacemaker implants[18–21].

MicroRNAs (miRNAs) are small, conserved, noncoding RNAs that are important components of post-transcriptional gene regulation and are involved in the control of many fundamental processes, including cardiac development and function. In particular, the expression of the miR-1 family, which comprises miR-1-1 and miR-1-2, is altered in mouse models and people with heart diseases[24–27]. Furthermore, overexpression of miR-1 in normal or infarcted rat heart exacerbates electrophysiological abnormalities[26], whereas ablation of the *miR-1-2* (*Mir1a-2*) gene in mice results in arrhythmias, cardiac conduction defects and sudden cardiac death[27], demonstrating that the heart needs tight regulation of miR-1. Here we set out to test whether or not miRNAs are misregulated in myotonic dystrophies.

RESULTS

The processing of miR-1 is altered in myotonic dystrophy

In a preliminary profiling analysis of the expression of miRNAs in primary differentiated muscle cells isolated from unaffected persons and those with DM1 (**Supplementary Fig. 1a,b** and **Supplementary Data**), we identified a robust misexpression of miR-1. Because inactivation of *miR-1-2* in mice did not result in an overt phenotype in

[1]Institut de Génétique et de Biologie Moléculaire et Cellulaire (IGBMC), Illkirch, France. [2]Institut National de la Santé et de la Recherche Médicale (INSERM) U964, Illkirch, France. [3]Centre National de la Recherche Scientifique (CNRS) UMR7104, Illkirch, France. [4]Strasbourg University, Illkirch, France. [5]Institut National de la Santé et de la Recherche Médicale U590, Lyon, France. [6]Necker Hospital, Paris, France. [7]Institut National de la Santé et de la Recherche Médicale U781, Paris, France. [8]Université Paris 5, Paris, France. [9]Cochin Hospital, Paris, France. [10]Université Pierre et Marie Curie (UM76), Paris, France. [11]Institut de Myologie, Paris, France. [12]Institut National de la Santé et de la Recherche Médicale U974, Paris, France. [13]Centre National de la Recherche Scientifique UMR7215, Paris, France. [14]University of Minnesota, Minneapolis, Minnesota, USA. [15]Department of Neurology, Toneyama Hospital, Osaka, Japan. [16]Department of Neurology, Osaka University Graduate School of Medicine, Osaka, Japan. Correspondence should be addressed to N.C.-B. (ncharlet@igbmc.fr).

Received 14 September 2010; accepted 7 April 2011; published online 19 June 2011; doi:10.1038/nsmb.2067

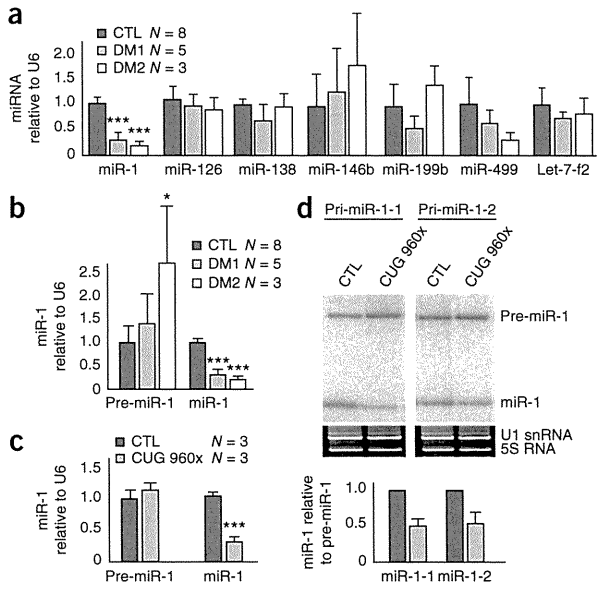

Figure 1 The processing of miR-1 is altered in myotonic dystrophies. (**a**) Quantitative real-time PCR (qRT-PCR) analysis of the expression of mature miR-1, miR-126, miR-138, miR-199 and miR-499 relative to the U6 small nuclear (sn) RNA in heart samples of adults with DM1 or DM2 and in control (CTL) heart samples from 2 unaffected persons, 1 person with dilated cardiomyopathy and 5 people with ALS. $^{***}P < 0.001$. (**b**) qRT-PCR analysis of the expression of pre-miR-1 and mature miR-1 relative to the U6 snRNA in heart samples of control (2 unaffected, 1 with dilated cardiomyopathy and 5 with ALS), DM1-affected and DM2-affected subjects. $^{*}P < 0.05$, $^{***}P < 0.001$. (**c**) qRT-PCR analysis of the expression of pre-miR-1 and mature miR-1 in H9C2 rat cardiomyocytes differentiated for 6 days and infected with recombinant adenovirus (MOI 100) expressing GFP (CTL) or 960 CUG repeats (CUG). The mean of at least three independent infections is depicted as the percentage of mature or pre-miR-1 relative to the U6 snRNA. Error bars indicate s.d. $^{***}P < 0.001$. (**d**) 5 μg of total RNA extracted from HeLa cells co-transfected with ectopic pri-miR-1-1 or pri-miR-1-2 minigenes and a plasmid expressing either no (CTL) or 960 CUG repeats (CUG) were analyzed by northern blot analysis using an antisense miR-1 [γ-^{32}P]–labeled probe. The mean of at least three independent transfections is depicted as the percentage of mature miR-1 relative to pre-miR-1. Ethidium bromide staining demonstrates equal loading. Error bars indicate s.d.

nonregenerating skeletal muscle but did cause cardiac dysfunction[27], we quantified miR-1 expression in heart samples from people with DM1 and in unaffected individuals. Quantitative RT-PCR demonstrated a significant reduction in expression of miR-1 ($P = 1.8 \times 10^{-6}$) in DM1 heart tissue (**Fig. 1a**), whereas the expression of miR-126, miR-138, miR-199, miR-208, miR-499 and Let-7-f2 was not altered. Additional northern blot analysis confirmed decreased expression of miR-1 in DM1 heart tissue (**Supplementary Fig. 1c**). Next, miR-1 expression was examined in myotonic dystrophy type 2, which undergoes cardiac alterations similar to those in DM1 (ref. 28). Quantitative RT-PCR demonstrated a significant ($P < 0.001$) reduction in expression of miR-1 in heart samples from people with DM1 and DM2 but no alteration in heart samples from those with amyotrophic lateral sclerosis (**Fig. 1a**), suggesting that the expression of miR-1 is specifically altered in both forms of myotonic dystrophy.

miRNAs are initially transcribed by RNA polymerase II as primary miRNAs (pri-miRNAs), which are processed into precursor miRNAs (pre-miRNAs) by Drosha complexed with DGCR8 (also called Pasha)[29–31] and exported from the nucleus to the cytoplasm by exportin 5 (XPO5)[32,33]. Pre-miRNAs are hairpin-shaped RNAs of approximately 70 nucleotides (nt) that are processed into mature miRNAs by Dicer[34,35], a cytoplasmic endoRNase of the RNase type III family. Expanded CUG or CCUG repeats interfere *in trans* with the alternative splicing of other pre-messenger RNAs[14–17]. To investigate whether expanded CUG or CCUG repeats also interfere *in trans* with the processing of miR-1 in myotonic dystrophic heart tissues, we quantified the expression of pre-miR-1 and mature miR-1. Whereas the levels of pre-miR-1 were normal or slightly increased, the quantities of mature miR-1 were decreased in heart samples of people with DM1 and people with DM2 (**Fig. 1b**), suggesting that pre-miR-1 is normally produced but incorrectly processed in individuals with myotonic dystrophy. In contrast, the expression of pre- and mature miR-138 and pre- and mature Let7-f2 were normal, indicating that the misregulation of the processing of pre-miR-1 was specific and was not the result of a global alteration of miRNA biogenesis (**Supplementary Fig. 1d**).

To test whether the expression of expanded CUG repeats directly altered the processing of pre-miR-1, we engineered an adenovirus expressing 960 expanded CUG repeats and infected rat H9C2 cardiomyocytes, which express endogenous miR-1. RNA FISH coupled to immunofluorescence analysis confirmed that >90% of the cardiomyocytes were infected and expressed expanded CUG repeats, which sequestered endogenous Mbnl1 within nuclear aggregates (**Supplementary Fig. 1e**). In CUG-infected cardiomyocytes, the expression of mature miR-1 was decreased, whereas that of pre-miR-1 was not altered (**Fig. 1c**). This misregulation of pre-miR-1 processing was specific, as the expression of mature and pre-miR-138 or of mature and pre-Let7-f2 was normal (**Supplementary Fig. 1f**). The miR-1 family includes two paralogs expressed in heart tissue, miR-1-1 and miR-1-2, encoded by two different genes but expressing identical mature miRNAs, which cannot be differentiated by northern blot or quantitative PCR with reverse transcription (RT-qPCR) (**Supplementary Fig. 1g**). To rule out any transcriptional regulation and to determine whether expanded CUG repeats alter the processing of pre-miR-1-1, pre-miR-1-2 or both, we cloned human pri-miR-1-1 and pri-miR-1-2 under the control of a cytomegalovirus (CMV) promoter. Coexpression of ectopic pri-miR-1-1 or pri-miR-1-2 minigene in HeLa cells, which do not express endogenous miR-1, with a vector expressing expanded CUG repeats altered both pre-miR-1-1 and pre-miR-1-2 processing, resulting in decreased expression of mature miR-1-1 and miR-1-2 (**Fig. 1d**). As a negative control, expression of expanded CUG repeats had no substantial effect on the processing of the ectopically expressed pre-miR-16 (**Supplementary Fig. 1h**). Overall, these data demonstrate that the processing of the miR-1 family is altered in the hearts of people with DM1 or DM2, and that expression of expanded CUG repeats is sufficient to trigger that alteration.

MBNL1 regulates the processing of miR-1

Because expanded CUG repeats alter MBNL1 and CUGBP1 functions, we tested whether these proteins regulate the processing of pre-miR-1. Depletion of MBNL1 by short hairpin RNA (shRNA) mimicked the action of CUG repeats and altered the processing of ectopically expressed pri-miR-1-1 or pri-miR-1-2 minigenes, resulting in lower quantities of mature miR-1-1 or miR-1-2 (**Fig. 2a** and data not shown). These results were confirmed with two other shRNAs directed against *MBNL1* (**Supplementary Fig. 2a**). In contrast, overexpression or depletion of CUGBP1 had little effect on

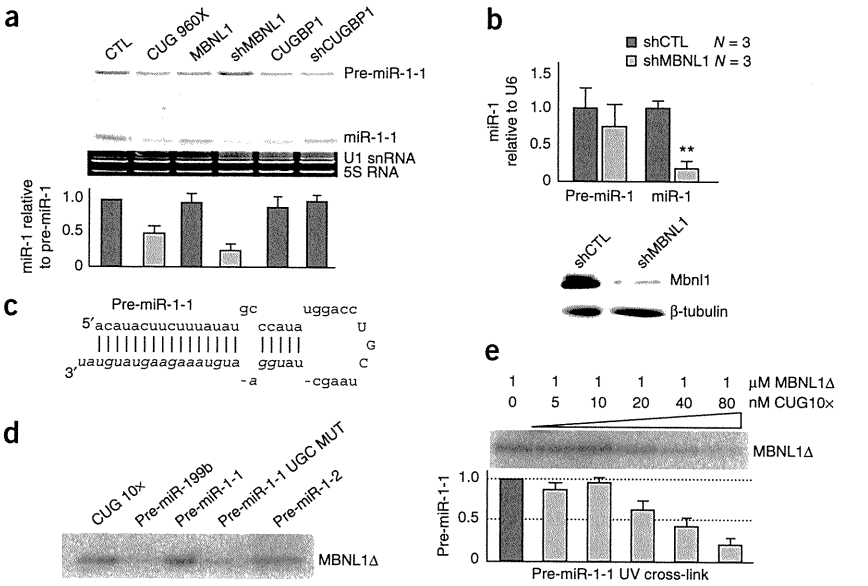

Figure 2 MBNL1 regulates the processing of miR-1. (**a**) Northern blot analysis of RNA extracted from HeLa cells co-transfected with ectopic pri-miR-1-1 minigene and a plasmid expressing either no CTG (CTL), 960 CUG repeats (CUG), MBNL1, CUGBP1 or shRNA directed against *MBNL1* (shMBNL1 #1) or against *CUGBP1* (shCUGBP1). The mean of at least three independent transfections is depicted as the percentage of mature miR-1 relative to pre-miR-1. Error bars indicate s.d., and ethidium bromide staining demonstrates equal loading. (**b**) Top, qRT-PCR analysis of the expression of endogenous pre-miR-1 and mature miR-1 in H9C2 rat cardiomyocytes infected with recombinant adenovirus expressing an shRNA against *LacZ* (shCTL) or against *Mbnl1* (shMBNL1). The mean of at least three independent infections is depicted as the percentage of mature or pre-miR-1 relative to the U6 snRNA. Error bars indicate s.d. $^{**}P < 0.01$. Bottom, Mbnl1 depletion was confirmed by western blotting. (**c**) Sequence of the wild-type human pre-miR-1-1. Mature miR-1 is indicated in italic. The UGC motif mutated in UAC is indicated in upper case. (**d**) UV-cross-linking analysis of pre-miR-1-1, pre-miR-1-2 and mutated pre-miR-1-1 (UGC MUT) using purified bacterial recombinant GST-MBNL1ΔCter and uniformly [α-^{32}P]CTP-labeled RNAs. (**e**) UV-cross-linking binding of GST-MBNL1ΔCter to uniformly [α-^{32}P]CTP-labeled pre-miR-1-1 RNA is competed by increasing amounts of unlabeled RNA composed of 10 CUG repeats. The mean of at least three independent experiments is depicted as the binding of MBNL1 to pre-miR-1. Error bars indicate s.d.

pre-miR-1 processing, suggesting that the sole depletion of MBNL1 is sufficient to mimic the action of expanded CUG repeats and to alter the processing of pre-miR-1. To test whether MBNL1 regulates the processing of endogenous pre-miR-1, we engineered an adenovirus expressing an shRNA directed against *Mbnl1* to transduce rat H9C2 cardiomyocytes. Depletion of Mbnl1 in cardiomyocytes resulted in a significantly decreased quantity of mature miR-1 ($P < 0.01$), whereas the expression of pre-miR-1 was not altered (**Fig. 2b**), suggesting that MBNL1 regulates the processing of endogenous pre-miR-1. Levels of endogenous miR-126, miR-138, miR-199 and Let-7-f2, which were tested as negative controls, were not altered, suggesting that MBNL1 specifically regulates the processing of pre-miR-1 (**Supplementary Fig. 2b**). Next, we found that recombinant purified glutathione *S*-transferase (GST)-tagged MBNL1 binds to pre-miR-1-1 and to pre-miR-1-2 RNAs, and—consistent with previous studies[36,37]—mutation of a UGC motif (**Fig. 2c**), which is located within the loop of pre-miR-1 and is conserved among species and miR-1 family members (**Supplementary Fig. 2c**), was sufficient to reduce MBNL1 binding in UV-cross-linking experiments (**Fig. 2d**), and in gel-shift analysis (**Supplementary Fig. 2d**). Finally, the binding of MBNL1 to pre-miR-1-1 RNA was outcompeted by an excess of unlabeled expanded CUG repeats (**Fig. 2e**), in accordance with the proposed model[14–17] of myotonic dystrophy pathogenesis, in which an excess of expanded CUG repeats reduces the quantity of free MBNL1 and consequently the binding of MBNL1 to its physiological targets.

LIN28 regulates the processing of miR-1

To determine the mechanism underlying the alteration of pre-miR-1 processing, we examined pre-miR-1 localization and cleavage but found that neither expanded CUG repeats nor MBNL1 had a detectable effect on pre-miR-1 export or on Dicer localization and activity (**Supplementary Fig. 3a** and data not shown). Recent reports demonstrated that the LIN28 and LIN28B RNA binding proteins regulate the expression of the Let-7 family of miRNA[38–41], raising the question of whether LIN28 may also regulate miR-1. Overexpression of LIN28 inhibited the processing of ectopically expressed pre-miR-1-1 or pre-miR-1-2, resulting in lower expression of mature miR-1-1 and miR-1-2 (**Fig. 3a**). Similar experiments conducted in the presence of actinomycin D, which inhibited *de novo* production of pre-miR-1, suggested that LIN28 blocked the processing of pre-miR-1 at the Dicer step (**Supplementary Fig. 3b**). To test whether LIN28 regulates the processing of endogenous pre-miR-1, rat H9C2 cardiomyoblastes were infected with lentiviral particles expressing an shRNA directed against *Lin28B* (*Lin28b*). Depletion of Lin28B stimulated the expression of endogenous mature miR-1, whereas the expression of pre-miR-1 was not substantially altered (**Fig. 3b**), confirming that LIN28 regulates the processing of pre-miR-1. Effect of Lin28B depletion was also tested on the expression of endogenous Let-7-f2 and miR-199, which were used as positive[38,39] and negative controls, respectively (**Supplementary Fig. 3c**). Similar to pre-Let7 miRNAs[40,41], recombinant purified histidine (His)-tagged LIN28 promoted *in vitro* uridylation of pre-miR-1 by immunoprecipitated Flag-tagged ZCCHC11 (also called TUT4) (**Fig. 3c** and **Supplementary Fig. 3d**). Consistent with the discovery that uridylation of pre-Let-7 blocks Dicer processing[41], uridylated pre-miR-1 was not cleaved by immunoprecipitated Myc-tagged Dicer, whereas control nonuridylated pre-miR-1 was processed into mature miR-1 (**Fig. 3d**). Next, using UV-cross-linking assays (**Fig. 3e**) and gel-shift analysis, we found that recombinant purified His-tagged LIN28 protein binds to pre-miR-1-1 and to pre-miR-1-2 RNAs, (**Supplementary Fig. 3e**). The pre-miR-1-1 loop possesses G- and A-rich motifs similar to the sequences recognized by LIN28 in the pre-Let-7-A1 loop[38], and mutation of an AAG motif in the pre-miR-1-1 loop reduced LIN28 binding (**Fig. 3e**). These data suggest that LIN28 and MBNL1 may bind the pre-miR-1 loop in a mutually exclusive pattern.

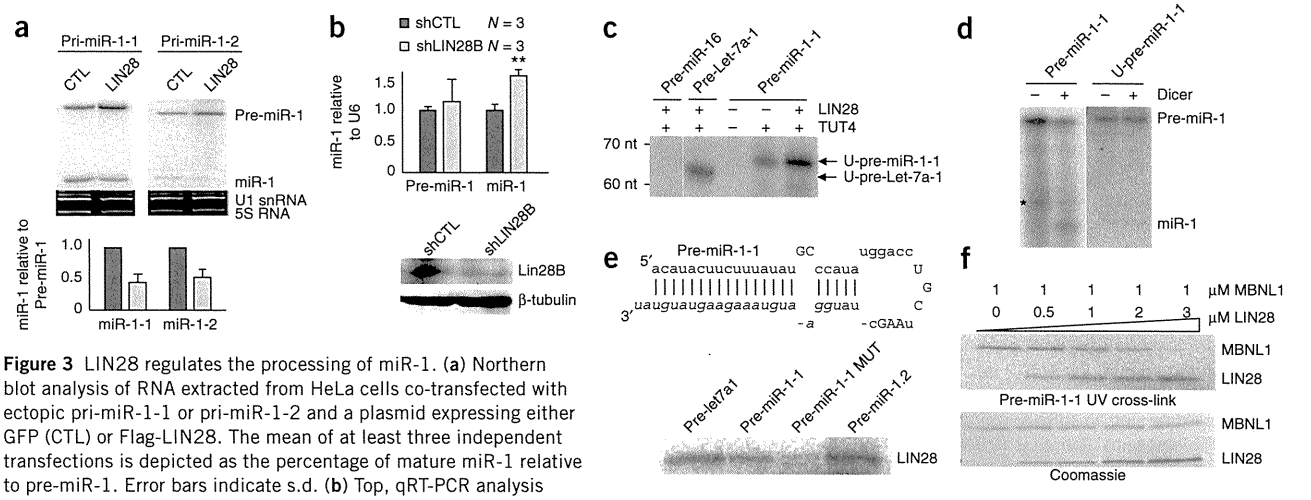

Figure 3 LIN28 regulates the processing of miR-1. (**a**) Northern blot analysis of RNA extracted from HeLa cells co-transfected with ectopic pri-miR-1-1 or pri-miR-1-2 and a plasmid expressing either GFP (CTL) or Flag-LIN28. The mean of at least three independent transfections is depicted as the percentage of mature miR-1 relative to pre-miR-1. Error bars indicate s.d. (**b**) Top, qRT-PCR analysis of the expression of endogenous pre-miR-1 and mature miR-1 in undifferentiated H9C2 rat cardiomyoblastes infected with recombinant lentivirus expressing an shRNA against *Gapdh* (shCTL) or against *Lin28B* (shLIN28B). The mean of at least three independent infections is depicted as the percentage of mature or pre-miR-1 relative to the U6 snRNA. Error bars indicate s.d. $^{**}P < 0.01$. Bottom, Lin28B depletion was confirmed by western blotting. (**c**) Immunoprecipitated Flag-TUT4 uridylates pre-miR-1-1 in presence of [α-^{32}P]UTP and 100 nM of His-LIN28. Pre-miR-16 and pre-Let-7-A1 are negative and positive controls, respectively. (**d**) Immunoprecipitated Myc-Dicer processes [γ-^{32}P]–labeled pre-miR-1 into mature miR-1 but does not cleave pre-miR-1 that was previously uridylated by TUT4 and LIN28. The asterisk (*) indicates a nonspecific degradation product. (**e**) Top, sequence of human pre-miR-1-1. Mature miR-1 is indicated in italics. Mutated UGC and AAG motifs are indicated in upper case (MUT). Bottom, UV-cross-linking analysis of pre-miR-1-1, pre-miR-1-2 and mutated pre-miR-1-1 (MUT) was conducted using purified His-LIN28 and uniformly [α-^{32}P]CTP-labeled RNAs. (**f**) UV-cross-linking binding of GST-MBNL1ΔCter to uniformly [α-^{32}P]CTP-labeled pre-miR-1-1 RNA is competed by the indicated increasing amounts of His-LIN28.

We confirmed this hypothesis and found that increasing amounts of recombinant purified LIN28 outcompeted MBNL1 binding to pre-miR-1-1 RNA (**Fig. 3f**). Both LIN28 and MBNL1 have been reported to be expressed in adult heart tissue[42,43], suggesting that competition may arise *in vivo*. Finally, we found that regulation of the processing of pre-miR-1 is a physiological process, which is controlled during rat H9C2 cardiomyocytes differentiation and correlates with a decreased expression of Lin28B (**Supplementary Fig. 3f**). This is consistent with splicing misregulation in myotonic dystrophy, which copies a undifferentiated state. Together, these data suggest that the LIN28 and ZCCHC11 pathway regulates the expression of miR-1 and that LIN28 and MBNL1 compete for binding to pre-miR-1-1, which implies that a reduction of free MBNL1 in myotonic dystrophy would enable LIN28 to bind and to downregulate pre-miR-1.

Targets of miR-1 are upregulated in myotonic dystrophy

Finally, miR-1 regulates the post-transcriptional expression of various targets[26,44–47], which brings into question the consequences and importance of misregulation of miR-1 for myotonic dystrophy. Analysis with miRanda (http://www.microrna.org/) predicted various targets of miR-1, including the cardiac L-type calcium channel gene *CACNA1C* (*CAV1.2*) (**Fig. 4a**). CACNA1C is the main calcium channel in heart tissue, and gain-of-function mutations in the *CACNA1C* gene result in arrhythmias and sudden death[48]. We confirmed that CACNA1C is regulated by miR-1, as co-transfection of miR-1 reduced the expression of a luciferase reporter plasmid containing part of the 3′ UTR sequences of *CACNA1C* (**Fig. 4b**). In addition, overexpression of miR-1 in H9C2 cardiomyoblasts reduced the level of endogenous CACNA1C protein, whereas an antisense RNA oligonucleotide directed against miR-1

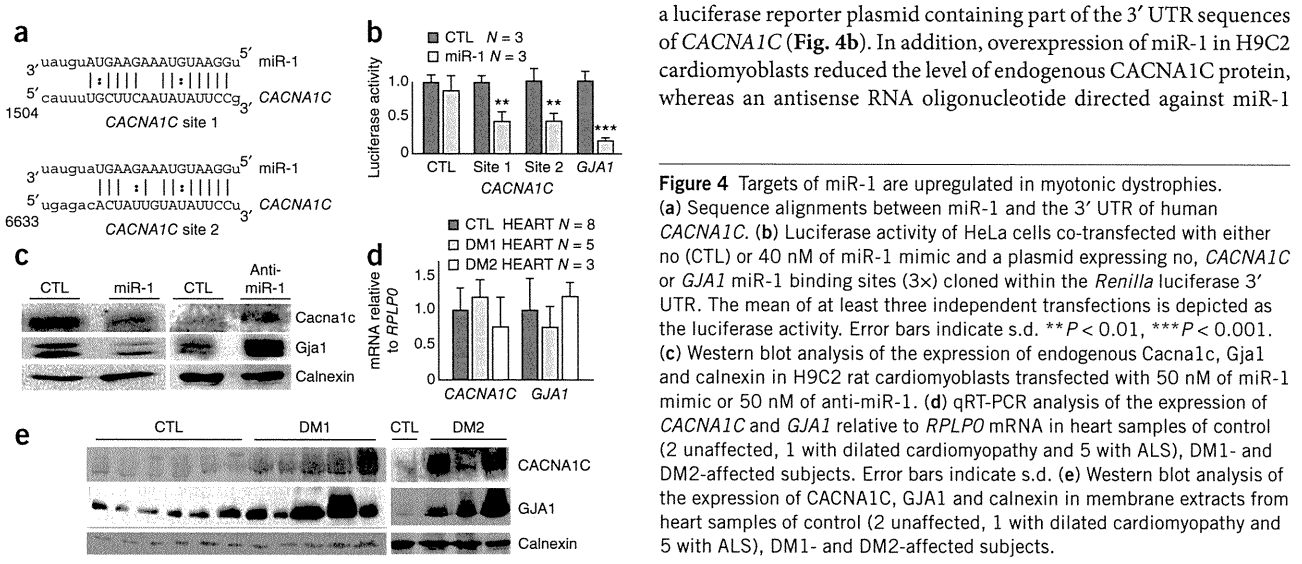

Figure 4 Targets of miR-1 are upregulated in myotonic dystrophies. (**a**) Sequence alignments between miR-1 and the 3′ UTR of human *CACNA1C*. (**b**) Luciferase activity of HeLa cells co-transfected with either no (CTL) or 40 nM of miR-1 mimic and a plasmid expressing no, *CACNA1C* or *GJA1* miR-1 binding sites (3×) cloned within the *Renilla* luciferase 3′ UTR. The mean of at least three independent transfections is depicted as the luciferase activity. Error bars indicate s.d. $^{**}P < 0.01$, $^{***}P < 0.001$. (**c**) Western blot analysis of the expression of endogenous Cacna1c, Gja1 and calnexin in H9C2 rat cardiomyoblasts transfected with 50 nM of miR-1 mimic or 50 nM of anti-miR-1. (**d**) qRT-PCR analysis of the expression of *CACNA1C* and *GJA1* relative to *RPLP0* mRNA in heart samples of control (2 unaffected, 1 with dilated cardiomyopathy and 5 with ALS), DM1- and DM2-affected subjects. Error bars indicate s.d. (**e**) Western blot analysis of the expression of CACNA1C, GJA1 and calnexin in membrane extracts from heart samples of control (2 unaffected, 1 with dilated cardiomyopathy and 5 with ALS), DM1- and DM2-affected subjects.

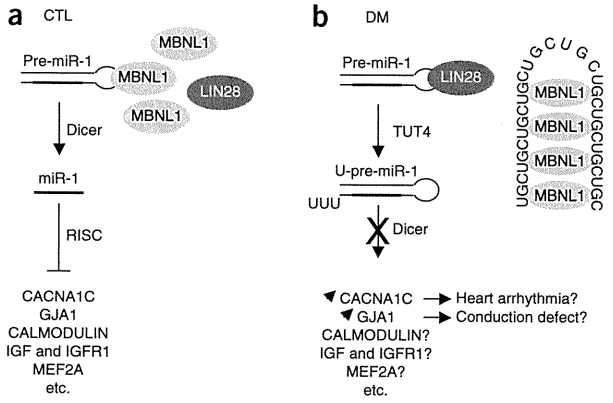

Figure 5 Model of miR-1 alteration in myotonic dystrophies. (**a**) MBNL1 and LIN28 compete for binding to pre-miR-1 loop. In presence of MBNL1, the processing of pre-miR-1 in mature miR-1 is favored and results in regulated expression of miR-1 targets. (**b**) In people with myotonic dystrophy, the sequestration of MBNL1 by expanded CUG or CCUG repeats allows LIN28 or LIN28B to bind to pre-miR-1, which promotes its consequent uridylation by TUT4. Uridylated pre-miR-1 is resistant to Dicer cleavage, which results in lower amounts of miR-1 and increased levels of its targets, GJA1 and CACNA1C.

increased the expression of endogenous CACNA1C (**Fig. 4c**). Notably, expression of CACNA1C protein was upregulated in DM1 and DM2 heart samples compared to control, whereas *CACNA1C* mRNA levels were not altered (**Fig. 4d,e**). Similarly, the expression of connexin 43 (GJA1), which is a known target of miR-1 (ref. 26) and is responsible for intracardiomyocyte conductance, was also upregulated at the protein level in heart samples of persons with DM1 or DM2 (**Fig. 4d,e**). These data demonstrate a post-transcriptional upregulation of miR-1 targets GJA1 and CACNA1C in people with myotonic dystrophy, which is consistent with a downregulation of the inhibitor, miR-1.

DISCUSSION

Our results suggest that mutant RNAs containing expanded CUG or CCUG repeats, which are known to modify the maturation of several pre-mRNAs, can also alter the processing of a pre-miRNA. Furthermore, we describe a previously unidentified function for MBNL1 as a cytoplasmic regulator of the biogenesis of pre-miR-1. Whether MBNL1 regulates the processing of other miRNAs remains to be determined, but we noted that UGC motifs are conserved in the loop of various pre-miRNAs (**Supplementary Table 1**). Furthermore, consistent with a report of LIN28 presence in the adult heart[42], our data suggest that the LIN28 and ZCCHC11 pathway regulates the processing of miR-1. We propose a model (**Fig. 5**) in which depletion of free MBNL1 by expanded CUG or CCUG repeats enables LIN28 and ZCCHC11 to uridylate pre-miR-1, which blocks Dicer processing, resulting in decreased expression of mature miR-1 and increased levels of its targets, including CACNA1C and GJA1, in the heart of people with myotonic dystrophy. GJA1 and CACNA1C encode the main gap junction and calcium channels in the heart, respectively, and we propose that their misregulation may contribute to the cardiac conduction defects and arrhythmias observed in people with DM1 or DM2 (**Fig. 5**). Whether other known (calmodulin[44], MEF2A[44], PP2A[45], IGF1 (ref. 46), TWF1 (ref. 47), etc.) or predicted (KCNA5, triadin, CUGBP2, etc.) targets of miR-1 are also upregulated in people with myotonic dystrophy remains to be determined. Furthermore, the miR-1 family regulates muscle-cell differentiation[49–53], which is delayed in the severe congenital DM1 form[54,55], suggesting that the alteration of pre-miR-1 processing may be involved in the manifestation of other symptoms of myotonic dystrophy. Finally, this work opens the possibility that the processing of specific miRNAs, which is highly regulated[56–59], can be altered and is involved in the development of human genetic diseases.

METHODS

Methods and any associated references are available in the online version of the paper at http://www.nature.com/nsmb/.

Note: Supplementary information is available on the Nature Structural & Molecular Biology website.

ACKNOWLEDGMENTS

We thank T. Cooper (Baylor College of Medicine) for the gift of the DT960 and tgCUGBP1 plasmids, C. Branlant (National Center of Scientific Research) for the pGEX-MBNL1-Δ101 (MBNL1ΔCter) vector, M. Swanson (University of Florida) for the pGEX-6P-MBNL1-His vector, C. Thornton (University of Rochester) for the polyclonal antibody against MBNL1, N. Kim (University of Seoul) for the pri-miR-16, Flag-TUT4, His-LIN28 and Flag-LIN28 plasmids, P. Provost (Université Laval) for the gift of the Myc-Dicer plasmid and all members of the French Myotonic Dystrophy Network for fruitful discussion. This work was supported by Institut National de la Santé et de la Recherche Médicale (INSERM) AVENIR (N.C.-B.), Agence nationale de la recherche (ANR) GENOPAT P007942 (N.C.B.), Association Française contre les Myopathies (AFM) MNM1-12982 (N.C.B.), the UPMC-emergence program (D.F), US National Institutes of Health (NIH) P30 AR057220 (J.W.D.), Muscular Dystrophy Center Core Laboratories (J.W.D.), the Ministère de l'enseignement supérieur et de la recherche and AFM (F.R., F.F.) and the University of Strasbourg (F.R., F.F.).

AUTHOR CONTRIBUTIONS

Experiments were conducted by F.R., F.F., C.F., J.-P.V., D.D., N.D., M.-C.F., A.N., D.A. and B.J. Clinical samples and patient data were obtained from J.W.D., D.D., K.W., D.F., G.G., H.F., D.D., M.P.T. and from the Research Resource Network supported by the Research Grant for Nervous and Mental Disorders from the Ministry of Health, Labour and Welfare, Japan. The study was designed and coordinated by N.D., D.F. and N.C.-B. The paper was written by N.C.-B.

COMPETING FINANCIAL INTERESTS

The authors declare no competing financial interests.

Published online at http://www.nature.com/nsmb/.
Reprints and permissions information is available online at http://www.nature.com/reprints/index.html.

1. Brook, J.D. *et al.* Molecular basis of myotonic dystrophy: expansion of a trinucleotide (CTG) repeat at the 3′ end of a transcript encoding a protein kinase family member. *Cell* **68**, 799–808 (1992).
2. Fu, Y.H. *et al.* An unstable triplet repeat in a gene related to myotonic muscular dystrophy. *Science* **255**, 1256–1258 (1992).
3. Mahadevan, M. *et al.* Myotonic dystrophy mutation: an unstable CTG repeat in the 3′ untranslated region of the gene. *Science* **255**, 1253–1255 (1992).
4. Liquori, C.L. *et al.* Myotonic dystrophy type 2 caused by a CCTG expansion in intron 1 of ZNF9. *Science* **293**, 864–867 (2001).
5. Miller, J.W. *et al.* Recruitment of human muscleblind proteins to (CUG)n expansions associated with myotonic dystrophy. *EMBO J.* **19**, 4439–4448 (2000).
6. Kanadia, R.N. *et al.* A muscleblind knockout model for myotonic dystrophy. *Science* **302**, 1978–1980 (2003).
7. Ho, T.H. *et al.* Muscleblind proteins regulate alternative splicing. *EMBO J.* **23**, 3103–3112 (2004).
8. Kanadia, R.N. *et al.* Reversal of RNA missplicing and myotonia after muscleblind overexpression in a mouse poly(CUG) model for myotonic dystrophy. *Proc. Natl. Acad. Sci. USA* **103**, 11748–11753 (2006).
9. Philips, A.V., Timchenko, L.T. & Cooper, T.A. Disruption of splicing regulated by a CUG-binding protein in myotonic dystrophy. *Science* **280**, 737–741 (1998).
10. Kuyumcu-Martinez, N.M. *et al.* Increased steady-state levels of CUGBP1 in myotonic dystrophy 1 are due to PKC-mediated hyperphosphorylation. *Mol. Cell* **28**, 68–78 (2007).
11. Mankodi, A. *et al.* Myotonic dystrophy in transgenic mice expressing an expanded CUG repeat. *Science* **289**, 1769–1773 (2000).
12. Lin, X. *et al.* Failure of MBNL1-dependent post-natal splicing transitions in myotonic dystrophy. *Hum. Mol. Genet.* **15**, 2087–2097 (2006).
13. Kalsotra, A. *et al.* A postnatal switch of CELF and MBNL proteins reprograms alternative splicing in the developing heart. *Proc. Natl. Acad. Sci. USA* **105**, 20333–20338 (2008).

14. Savkur, R.S. *et al.* Aberrant regulation of insulin receptor alternative splicing is associated with insulin resistance in myotonic dystrophy. *Nat. Genet.* **29**, 40–47 (2001).
15. Mankodi, A. *et al.* Expanded CUG repeats trigger aberrant splicing of ClC-1 chloride channel pre-mRNA and hyperexcitability of skeletal muscle in myotonic dystrophy. *Mol. Cell* **10**, 35–44 (2002).
16. Charlet-B., N. *et al.* Loss of the muscle-specific chloride channel in type 1 myotonic dystrophy due to misregulated alternative splicing. *Mol. Cell* **10**, 45–53 (2002).
17. Wheeler, T.M. *et al.* Correction of ClC-1 splicing eliminates chloride channelopathy and myotonia in mouse models of myotonic dystrophy. *J. Clin. Invest.* **117**, 3952–3957 (2007).
18. Groh, W.J. *et al.* Electrocardiographic abnormalities and sudden death in myotonic dystrophy type 1. *N. Engl. J. Med.* **358**, 2688–2697 (2008).
19. Pelargonio, G. *et al.* Myotonic dystrophy and the heart. *Heart* **88**, 665–670 (2002).
20. Phillips, M.F. & Harper, P.S. Cardiac disease in myotonic dystrophy. *Cardiovasc. Res.* **33**, 13–22 (1997).
21. Lazarus, A. *et al.* Long-term follow-up of arrhythmias in patients with myotonic dystrophy treated by pacing: a multicenter diagnostic pacemaker study. *J. Am. Coll. Cardiol.* **40**, 1645–1652 (2002).
22. Wang, G.S. *et al.* Elevation of RNA-binding protein CUGBP1 is an early event in an inducible heart-specific mouse model of myotonic dystrophy. *J. Clin. Invest.* **117**, 2802–2811 (2007).
23. Mahadevan, M.S. *et al.* Reversible model of RNA toxicity and cardiac conduction defects in myotonic dystrophy. *Nat. Genet.* **38**, 1066–1070 (2006).
24. Sayed, D. *et al.* MicroRNAs play an essential role in the development of cardiac hypertrophy. *Circ. Res.* **100**, 416–424 (2007).
25. Carè, A. *et al.* MicroRNA-133 controls cardiac hypertrophy. *Nat. Med.* **13**, 613–618 (2007).
26. Yang, B. *et al.* The muscle-specific microRNA miR-1 regulates cardiac arrhythmogenic potential by targeting GJA1 and KCNJ2. *Nat. Med.* **13**, 486–491 (2007).
27. Zhao, Y. *et al.* Dysregulation of cardiogenesis, cardiac conduction, and cell cycle in mice lacking miRNA-1–2. *Cell* **129**, 303–317 (2007).
28. Schoser, B.G. *et al.* Sudden cardiac death in myotonic dystrophy type 2. *Neurology* **63**, 2402–2404 (2004).
29. Lee, Y. *et al.* The nuclear RNase III Drosha initiates microRNA processing. *Nature* **425**, 415–419 (2003).
30. Denli, A.M. *et al.* Processing of primary microRNAs by the Microprocessor complex. *Nature* **432**, 231–235 (2004).
31. Han, J. *et al.* The Drosha-DGCR8 complex in primary microRNA processing. *Genes Dev.* **18**, 3016–3027 (2004).
32. Lund, E. *et al.* Nuclear export of microRNA precursors. *Science* **303**, 95–98 (2004).
33. Yi, R. *et al.* Exportin-5 mediates the nuclear export of pre-microRNAs and short hairpin RNAs. *Genes Dev.* **17**, 3011–3016 (2003).
34. Zhang, H. *et al.* Single processing center models for human Dicer and bacterial RNase III. *Cell* **118**, 57–68 (2004).
35. Chendrimada, T.P. *et al.* TRBP recruits the Dicer complex to Ago2 for microRNA processing and gene silencing. *Nature* **436**, 740–744 (2005).
36. Goers, E.S. *et al.* MBNL1 binds GC motifs embedded in pyrimidines to regulate alternative splicing. *Nucleic Acids Res.* **38**, 2467–2484 (2010).
37. Yuan, Y. *et al.* Muscleblind-like 1 interacts with RNA hairpins in splicing target and pathogenic RNAs. *Nucleic Acids Res.* **35**, 5474–5486 (2007).
38. Heo, I. *et al.* Lin28 mediates the terminal uridylation of let-7 precursor MicroRNA. *Mol. Cell* **32**, 276–284 (2008).
39. Rybak, A. *et al.* A feedback loop comprising lin-28 and let-7 controls pre-let-7 maturation during neural stem-cell commitment. *Nat. Cell Biol.* **10**, 987–993 (2008).
40. Hagan, J.P. *et al.* Lin28 recruits the TUTase Zcchc11 to inhibit let-7 maturation in mouse embryonic stem cells. *Nat. Struct. Mol. Biol.* **16**, 1021–1025 (2009).
41. Heo, I. *et al.* TUT4 in concert with Lin28 suppresses microRNA biogenesis through pre-microRNA uridylation. *Cell* **138**, 696–708 (2009).
42. Yang, D.H. & Moss, E.G. Temporally regulated expression of Lin-28 in diverse tissues of the developing mouse. *Gene Expr. Patterns* **3**, 719–726 (2003).
43. Kalsotra, A. *et al.* A postnatal switch of CELF and MBNL proteins reprograms alternative splicing in the developing heart. *Proc. Natl. Acad. Sci. USA* **105**, 20333–20338 (2008).
44. Ikeda, S. *et al.* MicroRNA-1 negatively regulates expression of the hypertrophy-associated calmodulin and Mef2a genes. *Mol. Cell. Biol.* **8**, 2193–2204 (2009).
45. Terentyev, D. *et al.* miR-1 overexpression enhances Ca^{2+} release and promotes cardiac arrhythmogenesis by targeting PP2A regulatory subunit B56α and causing CaMKII-dependent hyperphosphorylation of RyR2. *Circ. Res.* **104**, 514–521 (2009).
46. Elia, L. *et al.* Reciprocal regulation of microRNA-1 and insulin-like growth factor-1 signal transduction cascade in cardiac and skeletal muscle in physiological and pathological conditions. *Circulation* **120**, 2377–2385 (2009).
47. Li, Q. *et al.* Attenuation of microRNA-1 derepresses the cytoskeleton regulatory protein twinfilin-1 to provoke cardiac hypertrophy. *J. Cell Sci.* **123**, 2444–2452 (2010).
48. Splawski, I. *et al.* $Ca_V1.2$ calcium channel dysfunction causes a multisystem disorder including arrhythmia and autism. *Cell* **119**, 19–31 (2004).
49. Hirai, H. *et al.* MyoD regulates apoptosis of myoblasts through microRNA-mediated down-regulation of Pax3. *J. Cell Biol.* **191**, 347–365 (2010).
50. Chen, J.F. *et al.* microRNA-1 and microRNA-206 regulate skeletal muscle satellite cell proliferation and differentiation by repressing Pax7. *J. Cell Biol.* **190**, 867–879 (2010).
51. Cacchiarelli, D. *et al.* MicroRNAs involved in molecular circuitries relevant for the Duchenne muscular dystrophy pathogenesis are controlled by the dystrophin / nNOS pathway. *Cell Metab.* **12**, 341–351 (2010).
52. Chen, J.F. *et al.* The role of microRNA-1 and microRNA-133 in skeletal muscle proliferation and differentiation. *Nat. Genet.* **38**, 228–233 (2006).
53. Yan, D. *et al.* MicroRNA-1/206 targets c-Met and inhibits rhabdomyosarcoma development. *J. Biol. Chem.* **284**, 29596–29604 (2009).
54. Furling, D., Lemieux, D., Taneja, K. & Puymirat, J. Decreased levels of myotonic dystrophy protein kinase (DMPK) and delayed differentiation in human myotonic dystrophy myoblasts. *Neuromuscul. Disord.* **8**, 728–735 (2001).
55. Furling, D. *et al.* Defective satellite cells in congenital myotonic dystrophy. *Hum. Mol. Genet.* **10**, 2079–2087 (2001).
56. Guil, S. & Cáceres, J.F. The multifunctional RNA-binding protein hnRNP A1 is required for processing of miR-18a. *Nat. Struct. Mol. Biol.* **14**, 591–596 (2007).
57. Davis, B.N. *et al.* Smad proteins bind a conserved RNA sequence to promote microRNA maturation by Drosha. *Mol. Cell* **39**, 373–384 (2010).
58. Trabucchi, M. *et al.* The RNA-binding protein KSRP promotes the biogenesis of a subset of microRNAs. *Nature* **459**, 1010–1014 (2009).
59. Yang, W. *et al.* Modulation of microRNA processing and expression through RNA editing by ADAR deaminases. *Nat. Struct. Mol. Biol.* **13**, 13–21 (2006).

ONLINE METHODS

Samples. All samples were from heart left ventricles. Heart samples from unaffected persons (CTL #1 and #2) were purchased at Ambion and Stratagene, respectively. CTL #3 was from a person suffering from familial dilated cardiomyopathy. CTL #4–8 were from ALS-affected subjects described previously[60]. DM1 #1 was from a 45-year-old patient suffering from DM1 with an expansion of 166 CTG repeats in the blood who underwent a cardiac transplantation for end-stage heart failure and dilated cardiomyopathy with conduction system disease. DM1 #2–5 were from previously described subjects (DM1 #9–11 in ref. 60) with expansion of 4,300 (female, 58 years), 4,800 (male, 63 years), 5,800 (female, 56 years) and ~6,000 CTG repeats in the heart. Subjects with DM2 were described previously[28].

RT-qPCR. miRNAs RT-qPCR analyses were conducted using the miScript reverse transcription kit (Qiagen), the specific miScript primer and precursor assays (Qiagen) and an miScript Sybr green PCR kit (Qiagen) in a Lightcycler 480 (Roche) for 15 min at 94 °C, followed by 50 cycles of 15 s at 94 °C, 20 s at 55 °C and 20 s at 72 °C. U6 snRNA was used as the standard. *GJA1* (fwd: 5′-TTTCCATCCACTTGCACAATA3′, rev: 5′-GGCTTGATTCCCTGACT-3′) and *CACNA1C* (fwd: 5′-TTCGTGTCCCTCTTCAACC-3′, rev: 5′-GTTGCT CAAGGAGTTCCAGTA-3′) RT-qPCR analyses were conducted using the Transcriptor Reverse Transcriptase Kit (Roche) and the QuantiTect SYBR Green PCR kit (QIAGEN) in a Lightcycler 480 (Roche) for 15 min at 94 °C, followed by 50 cycles of 15 s at 94 °C, 20 s at 58 °C and 20 s at 72 °C. *RPLP0* (fwd: 5′-GAAGTCACTGTGCCAGCCCA-3′, rev: 5′-GAAGGTGTAATCCGTCTCCA-3′) was used as the standard. Data were analyzed using Lightcycler 480 analysis software and the 2ΔCt method.

Northern blotting. HeLa cells were co-transfected using JetPei (Polyplus) in DMEM, 1 g l^{-1} glucose, 5% fetal calf serum and gentamycin at 37 °C, 5% (v/v) CO_2. 24 h after transfection, total RNA was extracted using Tri Reagent, treated with DNase, extracted with phenol-chloroform and precipitated with ethanol. 5 μg of RNA were electrophoresed on a 12% acryl-urea gel, transferred on nylon membrane, prehybridized 90 min at 42 °C in 6× SSPE, 0.1% (v/v) SDS, 2× Denhardt, hybridized overnight at 42 °C with 50 ng of antisense miR-1 (5′-ATACATACTTCTTTACATTCCA-3′) or U6 snRNA (5′-ATA TGGAACGCTTCACGAATT-3′) [γ-^{32}P]ATP-labeled probe, washed three times in SSPE 6×, SDS 0.1% (v/v), and revealed using a Typhoon scanner.

Lentiviral and adenoviral infection of H9c2 cells. Lentivirus expressing an shRNA against LIN28B were ordered from OpenBiosystems (V3LHS_327847) H9C2 cells were grown in DMEM, 1 g l^{-1} glucose, 10% (v/v) fetal calf serum and gentamycin at 37 °C, 5% (v/v) CO_2 and infected at a multiplicity of infection (MOI) of 20 during 48 h. Adenovirus expressing shMBNL1 or 960 CUG repeats were cloned into pAD-DEST (Invitrogen) and produced according to manufacturer's instructions. H9C2 cells were grown in DMEM, 1 gl^{-1} glucose, 10% fetal calf serum and gentamycin at 37 °C, 5% (v/v) CO_2. Confluent H9C2 cells were differentiated for 6 d in DMEM, 1 gl^{-1} glucose, 2% v/v) horse serum and gentamycin at 37 °C, 5% (v/v) CO_2 and transduced with recombinant CUG)960x or shMBNL1 adenovirus (MOI 100). Medium was replaced 24 h after infection, and cells were analyzed 48 h after infection.

***In vitro* uridylation.** HeLa cells were collected 24 h after transfection with Flag-TUT4, incubated at 4 °C in 300 mM Nacl, 10 mM Tris, pH 8.0, 1% (v/v) Triton X-100 for 20 min, sonicated and centrifuged 10 min at 21,000*g* at 4 °C. Supernatant was incubated with 30 μl of anti-Flag M2 affinity gel (Sigma) with constant rotation for 2 h at 4 °C. Beads were washed 3 times in 200 mM KCl, 10 mM Tris, pH 8.0, and incubated with 5 pmol of synthetic pre-miR-16, pre-miR-1-1 or pre-Let-7a-1 RNA (Sigma), 3.2 mM $MgCl_2$ and 125 nM [α-^{32}P]UTP at 37 °C for 1 h and analyzed on 12% (v/v) acryl, 8 M urea gel.

***In vitro* Dicer processing.** HeLa cells were harvested 24 h after transfection with Myc-Dicer, incubated at 4 °C in lysis buffer (150 mM NaCl, 10 mM Tris, pH 8.0, 0.1% (v/v) Triton X-100) for 20 min, sonicated and centrifuged for 10 min at 21,000*g*. Supernatant was incubated with 30 μl of anti-Myc antibody bound to protein G–Sepharose with constant rotation for 2 h at 4 °C. Beads were washed three times in lysis buffer and incubated with [γ-^{32}P]ATP-labeled pre-miR-1-1 or previously uridylated pre-miR-1-1 in 6.4 mM $MgCl_2$, 1 mM DTT, for 30 min at 37 °C and analyzed in 12% (v/v) acrylamide, 8 M urea gel.

Luciferase assays. 40-nt fragments encompassing miR-1 binding sites within the 3′ UTR of human *CACNA1C* or *GJA1* were inserted in triplicate within the XbaI-NotI sites of pRLTK. HeLa cells were plated in a 24-well plate and transfected with 100 ng of luciferase vectors and 20 pmol of mimic miR-1 (Qiagen), using Lipofectamine2000 and assayed for luciferase activities 24 h after transfection, using the Dual Luciferase Reporter Assay kit (Promega).

Western blotting. Total- and membrane-protein extraction were done as previously described[17], and the product was separated on 7% (v/v) or 10% (v/v) SDS-PAGE gel, transferred onto nitrocellulose membranes, blocked with 5% (v/v) nonfat dry milk (NFM) in TBS, incubated with GJA1 (rabbit polyclonal, Sigma, 1:20,000), CACNA1C (rabbit polyclonal, Alomone, 1:100), MBNL1 (rabbit polyclonal, 1:100, gift from C. Thornton), LIN28B (rabbit polyclonal ab71415, Abcam) or calnexin (rabbit polyclonal, Stressgen, 1:1,000) antibody overnight in TBS and 5% (v/v) NFM, washed and incubated with Donkey anti-rabbit peroxidase antibody (Jackson Immunoresearch, 1:10,000) for 1 h in TBS and 5% (v/v) NFM, 0.1% (v/v) Tween 20, which was followed by autoradiographic revelation.

Additional methods. Information on miRNA expression profiling, bioinformatic analysis, RNA fluorescence *in situ* hybridization (FISH), immunofluorescence, recombinant protein production and purification, UV-cross-linking assays, gel-shift assay constructions and primer sequences is available in the **Supplementary Methods**.

60. Nakamori, M. *et al.* Aberrantly spliced α-dystrobrevin alters α-syntrophin binding in myotonic dystrophy type 1. *Neurology* **70**, 677–685 (2008).

doi:10.1038/nsmb.2067

Misregulated alternative splicing of *BIN1* is associated with T tubule alterations and muscle weakness in myotonic dystrophy

Charlotte Fugier[1,17], Arnaud F Klein[2,17], Caroline Hammer[1,17], Stéphane Vassilopoulos[2], Ylva Ivarsson[3], Anne Toussaint[1], Valérie Tosch[1], Alban Vignaud[2], Arnaud Ferry[2], Nadia Messaddeq[1], Yosuke Kokunai[4], Rie Tsuburaya[5], Pierre de la Grange[6], Doulaye Dembele[1], Virginie Francois[2], Guillaume Precigout[2], Charlotte Boulade-Ladame[7], Marie-Christine Hummel[1], Adolfo Lopez de Munain[8], Nicolas Sergeant[9], Annie Laquerrière[10], Christelle Thibault[1], François Deryckere[7], Didier Auboeuf[11], Luis Garcia[2], Pascale Zimmermann[3], Bjarne Udd[12–14], Benedikt Schoser[15], Masanori P Takahashi[4], Ichizo Nishino[5], Guillaume Bassez[16], Jocelyn Laporte[1], Denis Furling[2] & Nicolas Charlet-Berguerand[1]

Myotonic dystrophy is the most common muscular dystrophy in adults and the first recognized example of an RNA-mediated disease. Congenital myotonic dystrophy (CDM1) and myotonic dystrophy of type 1 (DM1) or of type 2 (DM2) are caused by the expression of mutant RNAs containing expanded CUG or CCUG repeats, respectively. These mutant RNAs sequester the splicing regulator Muscleblind-like-1 (MBNL1), resulting in specific misregulation of the alternative splicing of other pre-mRNAs. We found that alternative splicing of the bridging integrator-1 (*BIN1*) pre-mRNA is altered in skeletal muscle samples of people with CDM1, DM1 and DM2. BIN1 is involved in tubular invaginations of membranes and is required for the biogenesis of muscle T tubules, which are specialized skeletal muscle membrane structures essential for excitation-contraction coupling. Mutations in the *BIN1* gene cause centronuclear myopathy, which shares some histopathological features with myotonic dystrophy. We found that MBNL1 binds the *BIN1* pre-mRNA and regulates its alternative splicing. *BIN1* missplicing results in expression of an inactive form of BIN1 lacking phosphatidylinositol 5-phosphate–binding and membrane-tubulating activities. Consistent with a defect of BIN1, muscle T tubules are altered in people with myotonic dystrophy, and membrane structures are restored upon expression of the normal splicing form of BIN1 in muscle cells of such individuals. Finally, reproducing *BIN1* splicing alteration in mice is sufficient to promote T tubule alterations and muscle weakness, a predominant feature of myotonic dystrophy.

Myotonic dystrophy is the most common adult-onset muscular dystrophy and comprises two genetically distinct forms: DM1, which is caused by a CTG repeat expansion ranging from ~50 to 1,000 repeats in the 3′ untranslated region of the dystrophia myotonica-protein kinase (*DMPK*) gene[1–3], and DM2, which is caused by expansions of CCTG repeats in the first intron of the *CNBP* (also known as *ZNF9*) gene[4]. Furthermore, CTG expansions over 1,000 repeats are associated with the severe congenital form, CDM1.

Expression of RNAs containing expanded CUG or CCUG repeats interfere with the splicing of other pre-mRNAs through pathological alteration of two classes of RNA binding proteins[5–7]. MBNL1 is sequestered within nuclear RNA aggregates formed by expanded CUG and CCUG repeats[8–10] in individuals with CDM1, DM1 and DM2, whereas expression and phosphorylation of the CUG-binding protein-1 (CUGBP1) have been reported to be increased in individuals with DM1 (ref. 11). MBNL1 and CUGBP1 are RNA splicing factors, and altering their functional levels in myotonic dystrophic tissues results in reversion to embryonic splicing patterns for several mRNAs, such as the muscle chloride channel *CLCN1* and the insulin receptor *INSR*, resulting in myotonia and insulin resistance, respectively[12–14].

However, the cause of the progressive muscle weakness, which is a cardinal symptom of myotonic dystrophy, remains ill defined. Notably, the histopathological features of individuals with CDM1 (muscle fiber atrophy with centrally located nuclei in absence of regeneration) are similar to those of centronuclear myopathy (CNM)[15]. CNM's are caused by mutations in the myotubularin (*MTM1*), dynamin-2 (*DNM2*) and *BIN1* genes[16–18]. BIN1, also known as amphiphysin 2,

[1]Institut de Génétique et de Biologie Moléculaire et Cellulaire (IGBMC), Institut National de la Santé et de la Recherche Médicale (INSERM) U964, Centre National de la Recherche Scientifique (CNRS) UMR7104, University of Strasbourg, Illkirch, France. [2]Université Pierre et Marie Curie, University Paris 06, UM76, Institut de Myologie, INSERM U974 and CNRS UMR7215, Paris, France. [3]Department of Human Genetics, KU Leuven, Leuven, Belgium. [4]Department of Neurology, Osaka University Graduate School of Medicine, Osaka, Japan. [5]National Center of Neurology and Psychiatry, Tokyo, Japan. [6]GenoSplice technology, Hôpital Saint-Louis, Paris, France. [7]CNRS UMR7175, Université Louis Pasteur, Oncoprotéines, Ecole Supérieure de Biotechnologies de Strasbourg, Illkirch, France. [8]Hospital Donostia, Biodonostia Institute, Centro de Investigación Biomédica en Red sobre Enfermedades Neurodegenerativas–Instituto Carlos III, San Sebastián, Spain. [9]INSERM U837-1, Jean Pierre Aubert Research Center, Alzheimer and Tauopathies, Lille, France. [10]Pathology Laboratory, University Hospital of Rouen, Rouen, France. [11]INSERM U590, Centre Léon Bérard, Lyon, France. [12]Neuromuscular Research Center, Tampere University, Tampere, Finland. [13]Folkhälsan Institute of Genetics, Department of Medical Genetics, Helsinki University, Helsinki, Finland. [14]Department of Neurology, Vasa Central Hospital, Vasa, Finland. [15]Friedrich Baur Institute, Ludwig Maximilian University, Munich, Germany. [16]INSERM U955, Institut Mondor de Recherche Biomédicale, Créteil, France. [17]These authors contributed equally to this work. Correspondence should be addressed to N.C.-B. (ncharlet@igbmc.fr).

Received 28 December 2010; accepted 6 April 2011; published online 29 May 2011; doi:10.1038/nm.2374

is a protein specialized in membrane curvature whose function is regulated by alternative splicing (**Fig. 1a** and **Supplementary Fig. 1**). In skeletal muscles, inclusion of the muscle-specific exon 11, which encodes a phosphoinositide-binding domain[19], generates an isoform of BIN1 that induces tubular invaginations of membranes[19,20] and is implicated in T tubule biogenesis[19–21]. The T tubule network is a specialized membrane structure fundamental for excitation-contraction coupling in skeletal muscle, and disruption of *BIN1* in *Drosophila melanogaster* leads to disorganization of these structures and the dysfunction of the associated excitation-contraction coupling machinery[21].

Using whole-genome microarrays, we identified a robust misregulation of alternative splicing of the *BIN1* pre-mRNA in primary cultures of differentiated CDM1 muscle cells (**Supplementary Fig. 1a**). RT-PCR confirmed that exon 11 of *BIN1* mRNA was mostly skipped in skeletal muscles of individuals with myotonic dystrophy and that *BIN1* misregulation correlated with disease severity, as *BIN1* exon 11 was absent in severe congenital CDM1 but partially skipped in the milder adult DM1 and DM2 forms (**Fig. 1b,c**). As described for other misregulated splicing events identified in individuals with myotonic dystrophy, the skipping of *BIN1* exon 11 was also observed in embryonic skeletal muscles of control individuals (**Supplementary Fig. 1d,e**), suggesting that myotonic dystrophy may result from the failure to complete the developmental switch of a specific set of alternative splicing events.

Note that the misregulation of *BIN1* alternative splicing was specific to myotonic dystrophy, as we did not find it in muscle samples from people with amyotrophic lateral sclerosis (**Fig. 1c**). And it did not result from a global alteration of the splicing machinery, as we found no splicing alterations of *MTM1*, *DNM2* and *BIN1* brain-specific exons 13 to 16 in muscle samples from individuals with DM1 (data not shown). Finally, western blot analysis showed a reduction in the BIN1 protein isoform containing exon 11 in individuals with CDM1 and confirmed that this splicing misregulation did not alter the global level of BIN1 protein expression (**Fig. 1d**).

To determine the mechanisms underlying alterations of *BIN1* splicing, we constructed a minigene containing the exon 11 of *BIN1* bordered by its intronic regions and concurrently expressed it with a separate vector expressing only expanded CUG or CCUG repeats. Overexpression of ~1,000 CUG or 300 CCUG repeats repressed exon 11 inclusion, whereas the expression of a control plasmid containing the 3′ untranslated region of *DMPK* with no CTG repeats had no effect (**Fig. 2a**), indicating that expression of CUG or CCUG repeats was sufficient to induce *BIN1* splicing alteration. Depletion of MBNL1 by an siRNA-mediated approach mimicked the effect of CUG or CCUG repeats and promoted exon 11 exclusion, whereas overexpression of MBNL1 stimulated exon 11 inclusion (**Fig. 2a**). In contrast, overexpression or depletion of CUGBP1 had little effect on exon 11 inclusion (**Fig. 2a**). Similar dichotomous results between the effects of overexpression of MBNL1 and CUGBP1 have been reported with *INSR*, *CLCN1*, troponin T type 3 (skeletal, fast) (*Tnnt3*) and ATPase, Ca^{2+} transporting, cardiac muscle, fast twitch-1 (*ATP2A1*) minigenes[22–25], and only a subset of splicing events are co-regulated by CUGBP1 and MBNL1 (ref. 26), suggesting that the sole sequestration of MBNL1 is sufficient to induce splicing misregulation in myotonic dystrophy[27]. Consistent with the crystal structure of MBNL1 zinc fingers[28], MBNL1 recognized single-stranded UGC RNA motifs located downstream of *BIN1* exon 11 (**Fig. 2b** and **Supplementary Fig. 2b**). Mutation of MBNL1 binding sites reduced the responsiveness of the *BIN1* minigene to MBNL1, but also to expanded CUG or CCUG repeats (**Fig. 2c**), indicating that the *trans*-dominant effect of expanded CUG and CCUG repeats on splicing misregulation requires functional MBNL1 binding sites. Finally, binding of MBNL1 to the UGC motifs present in intron 11 of *BIN1* was competed by an excess of unlabeled expanded CUG repeats (**Fig. 2d**), which is consistent with the model of myotonic dystrophy in which an excess of expanded CUG or CCUG repeats reduces the quantity of free MBNL1 and, consequently, the binding of MBNL1 to its physiological RNA targets.

BIN1 protein is involved in membrane binding and curvature[19–21], and its muscle-specific exon 11 encodes a phosphoinositide-binding domain[19]. To investigate the consequences of *BIN1* exon 11 skipping for myotonic dystrophy, we first examined the tubulating activity of BIN1. As previously observed[18–21], overexpression of a plasmid containing the EGFP-tagged normal muscle splicing form of BIN1 (with exon 11) in C2C12 differentiated muscle cells induced the formation of

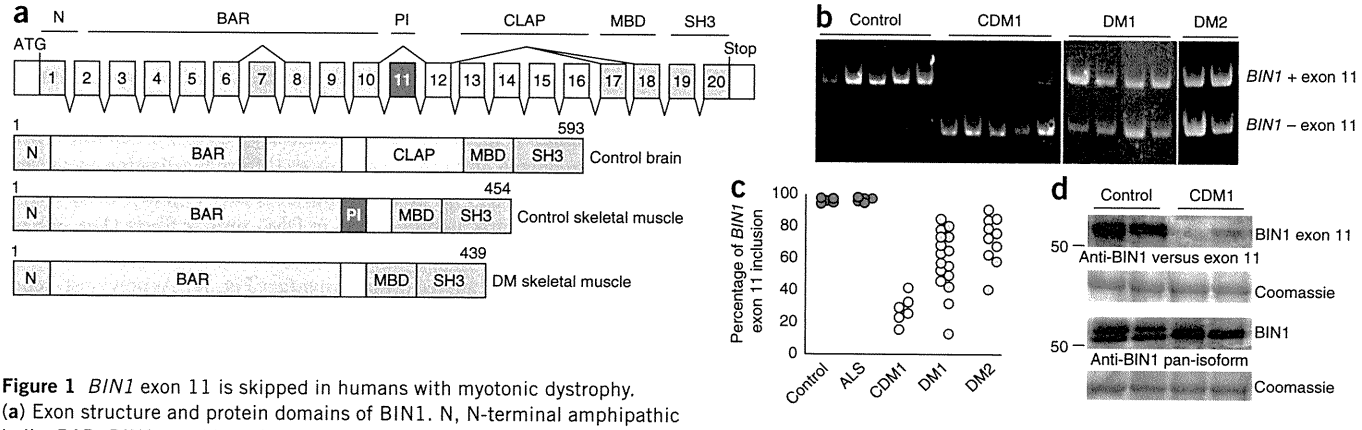

Figure 1 *BIN1* exon 11 is skipped in humans with myotonic dystrophy. (**a**) Exon structure and protein domains of BIN1. N, N-terminal amphipathic helix; BAR, BIN1-amphiphysin-Rvs167; PI, phosphoinositide-binding domain; CLAP, clathrin-associated protein–binding domain; MBD, Myc-binding domain; SH3, Src homology 3. The skeletal muscle–specific splicing form of BIN1 lacks the brain-specific CLAP domain but includes the muscle-specific PI-binding domain encoded by exon 11. (**b**) Representative RT-PCR analysis of endogenous *BIN1* mRNA from human skeletal muscle biopsies of normal adult individuals (control), fetuses with CDM1, and adults with DM1 and DM2. (**c**) Graphical representation of the RT-PCR analysis depicting the percentage of *BIN1* mRNA including exon 11 in skeletal muscle samples from normal individuals and individuals with amyotrophic lateral sclerosis (ALS), CDM1 (fetuses from 20 weeks to birth), DM1 (infants and adults) and DM2 (adults). (**d**) Representative western-blotting analysis of endogenous BIN1 protein from skeletal muscle samples of normal and age-matched fetuses with CDM1. Top, BIN1 was detected with an antibody directed against exon 11 (Anti-BIN1 versus exon 11). Middle, BIN1 was detected with the pan-isoform antibody directed against exon 17 (Anti-Bin1 pan-isoform). Equal loading was monitored by Coomassie staining. Similar results were obtained in four independent experiments.

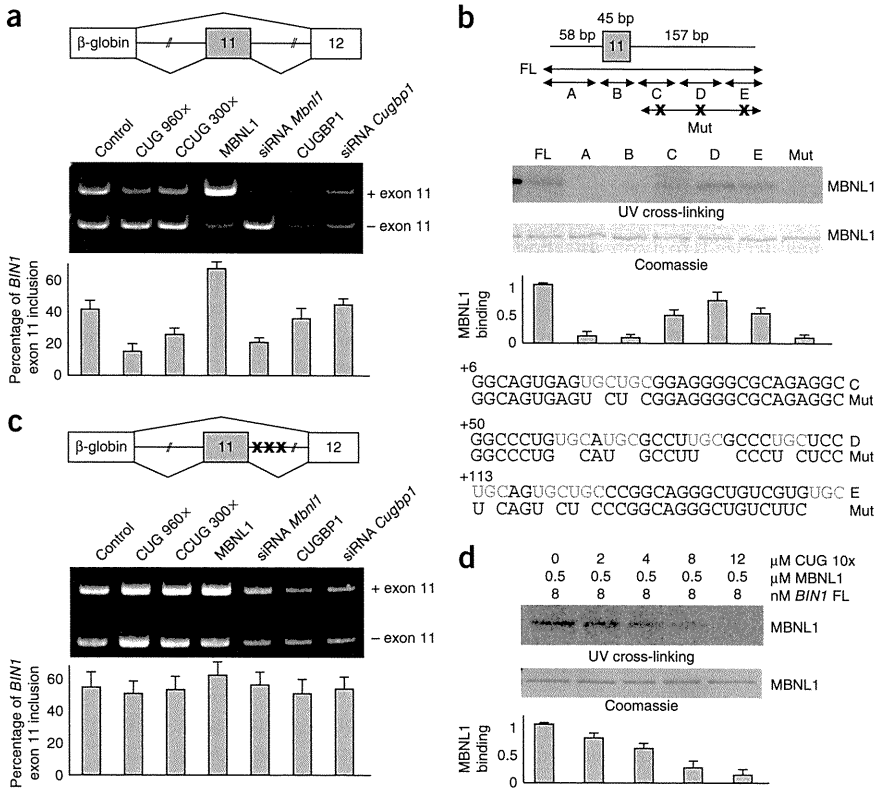

Figure 2 MBNL1 stimulates inclusion of *BIN1* exon 11. (**a**) Top, a schematic showing a *BIN1* minigene containing exon 11 bordered by 235 nucleotides of its upstream intron 10 and 226 nucleotides of its downstream intron 11. Middle, RT-PCR analysis of this minigene coexpressed with a plasmid expressing a *DMPK* minigene lacking CUG repeats (control), expressing 960 CUG repeats, 300 CCUG, GFP-MBNL1 or GFP-CUGBP1 or with siRNA directed against *Mbnl1* or against *Cugbp1* in C2C12 cells differentiated 24 h. Bottom, the mean of at least three independent transfections is depicted as the percentage of mRNA containing *BIN1* exon 11. Error bars indicate s.d. (**b**) Top, the RNAs derived from the *BIN1* minigene include nonoverlapping segments (A–E) of 58, 45, 43, 51 and 63 nucleotides, respectively. Middle, UV cross-linking assays done with 0.5 μg of purified bacterial recombinant GST-MBNL1Δ and RNAs uniformly labeled with ^{32}P-CTP. PhosphorImager exposition, Coomassie staining and quantification of at least three independent UV cross-linking assays are depicted as the intensity of MBNL1 binding relative to *BIN1* full-length (FL) RNA. Bottom, sequences of the wild-type and mutant RNAs used in the UV cross-linking experiments. (**c**) A *BIN1* minigene containing mutations of the UCG motifs in the downstream intron, analyzed as in **a**. (**d**) UV cross-linking binding of 0.5 μg of purified bacterial recombinant GST-MBNL1Δ to full-length *BIN1* RNA uniformly labeled with ^{32}P-CTP and competed by increasing amounts of unlabeled RNA containing ten CUG repeats. PhosphorImager exposition, Coomassie staining and quantification of three independent UV cross-linking assays are depicted as the intensity of MBNL1 binding relative to *BIN1* full-length RNA. Error bars in **a**–**d** indicate s.d.

numerous narrow tubular membrane structures (**Fig. 3a**). In contrast, expression of the splicing isoform of BIN1 (without exon 11) found in individuals with myotonic dystrophy produced little to no tubules, resulting in a diffuse cytoplasmic localization of BIN1 (**Fig. 3a**). We obtained identical results in nonmuscle cells (**Supplementary Fig. 3a**). Next, we tested the phosphoinositide-binding activity of the splicing forms of BIN1 containing or excluding exon 11. Lipid dot-blot assays (**Supplementary Fig. 3b**) and surface plasmon resonance experiments (**Fig. 3b**) showed that GST-tagged purified recombinant protein of the normal muscle isoform of BIN1 (with exon 11) recognized with high affinity phosphatidylinositol-5-phosphate (PtdIns5P) and phosphatidylinositol-3-phosphate (PtdIns3P) compared to phosphatidylinositol-4,5-biphosphate (PtdIns(4,5)P2) (apparent K_d values of 620 ± 20 nM, 660 ± 60 nM and 1,100 ± 100 nM, respectively). In contrast, the isoform of BIN1 found in individuals with myotonic dystrophy (without exon 11) had lost most of its ability to bind phosphoinositides (**Fig. 3b** and **Supplementary Fig. 3b**).

The similar affinity of BIN1 with exon 11 for PtdIns5P and PtdIns3P *in vitro* raises the question of whether BIN1 recognizes both phosphoinositides in cell culture. Transduction of muscle cell primary cultures with adenovirus expressing an EGFP-tagged probe for PtdIns5P, PtdIns3P or PtdIns(4,5)P2 revealed that the normal BIN1 isoform (with exon 11) colocalized with tubule structures containing PtdIns5P but not with endosomal vesicles containing PtdIns3P or with the plasma membrane enriched in PtdIns(4,5)P2 (**Supplementary Fig. 3c**), suggesting that BIN1 recognizes mostly PtdIns5P in muscle cells. Because mutations in the *MTM1* gene, which codes for the phosphatase responsible of PtdIns5P production[29], cause CNM[16], we propose that this phosphoinositide is enriched in BIN1-membrane structures and may constitute a functional link between BIN1 and MTM1.

The alteration of the activities of BIN1 *in vitro* and in cell culture made us wonder whether BIN1 functions are also altered in humans with myotonic dystrophy. In skeletal muscle, BIN1 is involved in the organization of the T tubule network[19–21], a specialized membrane structure fundamental for excitation-contraction coupling. As noted previously[19,21], immunofluorescence analysis of control human muscles showed that BIN1 was organized in transversal projections, which localized with the L-type calcium channel CACNA1S (also known as DHPRα1 or CAV1.1), a major component of T tubules (**Fig. 3c** and **Supplementary Fig. 3d**). In contrast, BIN1 was disorganized and presented a more diffuse localization in age-matched DM1 muscles (**Fig. 3c** and **Supplementary Fig. 3e**). CACNA1S localization was also slightly altered in DM1 muscle fibers (**Fig. 3c**), whereas labeling of ACTN1 (α-actinin-1), which is a marker of muscle fiber Z lines, was not altered (**Supplementary Fig. 3e**). As previously reported[30], ultrastructural analysis confirmed alterations of the T tubule network in DM1 muscles, with the presence of irregular and longitudinally orientated T tubules (**Fig. 3d**). Consistent with an alteration of BIN1 function, we observed a diffuse cytoplasmic localization of BIN1 and no or few BIN1 tubules in differentiated muscle cells isolated from humans with CDM1 and DM1 compared to control myotubes (**Fig. 3e**).

To test whether the absence of BIN1 structures observed in myotonic dystrophic muscle cells can be restored, we transduced CDM1 myotubes with an adenovirus expressing either the isoform of BIN1 found in normal individuals (with exon 11) or in individuals with myotonic dystrophy (without exon 11). Control BIN1 induced numerous BIN1 tubules in CDM1 myotubes, whereas expression of the splicing

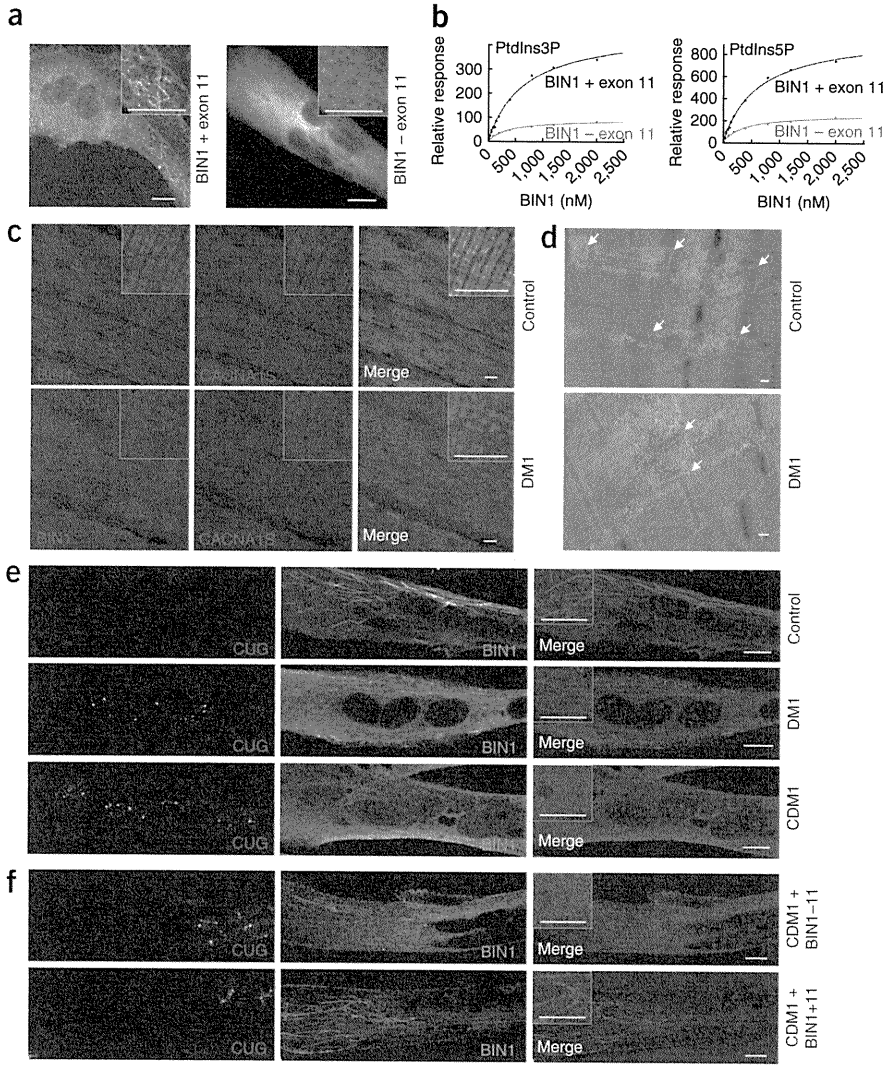

Figure 3 The splicing form of BIN1 expressed in myotonic dystrophic patients is inactive. (**a**) Representative images from confocal projections of differentiated C2C12 cells transfected with a plasmid expressing EGFP-BIN1 including or excluding exon 11. Insets, higher magnifications of GFP-BIN1 localization. Scale bars, 10 μm. (**b**) Surface plasmon resonance equilibrium titrations of full-length GST-BIN1 including or excluding exon 11 binding to 5% PtdIns5P and PtdIns3P in dioleoylphosphatidylcholine (DOPC) liposomes. The data were fitted by nonlinear regression analysis to the Langmuir binding isotherm. (**c**) Representative confocal images of immunofluorescence labeling of BIN1 and CACNA1S in paraffin-embedded longitudinal sections of skeletal muscles from an adult with DM1 and an age-matched control individual. Insets, higher magnifications of BIN1 and CACNA1S localizations. Scale bars, 10 μm. (**d**) Representative electron microscopy images of longitudinal sections of skeletal muscle from an adult with DM1 and an age-matched control individual. White arrows indicate T tubule structures. Scale bars, 100 nm. (**e**) Representative confocal images of RNA fluorescence *in situ* hybridization (FISH) using a Cy3-(CAG)7x PNA probe to detect CUG aggregates coupled to immunofluorescence detection of BIN1 of 6-d differentiated human skeletal muscle cells originating from a control individual, a person with DM1 (1,300 CTG repeats) and a person with CDM1 (2,000 CTG repeats). Nuclei are labeled by DAPI (blue) staining. Insets, higher magnifications of BIN1 localization. Scale bars, 10 μm. (**f**) Representative confocal images of RNA FISH labeling of CUG expanded repeats in CDM1 differentiated skeletal muscle cells transduced (multiplicity of infection of 1,500) with recombinant adenovirus expressing cDNA constructs of GFP-BIN1 containing or excluding exon 11. Insets, higher magnifications of GFP-BIN1 localization. Scale bars, 10 μm.

variant of BIN1 found in people with myotonic dystrophy did not (**Fig. 3f** and **Supplementary Fig. 3f**). Overall, these results indicate that the myotonic dystrophic splicing form of BIN1, which lacks exon 11, has lost most of its membrane binding and tubulating properties, and they suggest that T tubules are misorganized in myotonic dystrophic skeletal muscles and that expression of the normal splice form of BIN1 is sufficient to induce normal membrane structures.

Various altered splicing events have been reported in myotonic dystrophy, making unclear the importance of BIN1 misregulation. To test the consequences of the splicing alteration of *BIN1*, we artificially forced the skipping of *Bin1* exon 11 in mouse skeletal muscle through an exon-skipping strategy[31]. We cloned a modified U7 small nuclear RNA construct harboring an antisense sequence (U7-ex11AS), which specifically promoted skipping of *Bin1* exon 11 (**Fig. 4a** and **Supplementary Fig. 4a**), into an adeno-associated virus backbone (AAV2/1). We injected tibialis anterior muscles of wild-type newborn mice with U7-ex11AS virus, whereas we injected contralateral muscles with vehicle alone or with control AAV2/1. We analyzed the muscles 4 months after injection. Expression of U7-ex11AS reproduced the splicing alteration of *BIN1* observed in humans with myotonic dystrophy but did not induce other splicing changes (**Fig. 4b**), suggesting that this AAV2/1 exon 11 skipping strategy did not induce a global embryonal re-adaptation or any severe muscle degeneration or regeneration changes. Immunofluorescence analysis revealed that artificial skipping of *Bin1* exon 11 promoted Bin1 mislocalization and slight alterations of Cacna1s organization (**Fig. 4c**) compared to control-injected contralateral muscles. Markers of muscle Z lines, such as α-actinin and desmin, were not altered in U7-ex11AS–injected or control AAV2/1–injected muscles (data not shown), indicating that muscle integrity was maintained. Further histopathological and ultrastructural analyses revealed no major atrophy or degeneration of muscle fibers and normal mitochondrion and sarcomere structures (**Fig. 4d** and **Supplementary Fig. 4b**). In contrast, osmium tetroxide–potassium ferricyanide staining showed that ~30% of T tubules were abnormal in *Bin1* exon 11–skipped muscles, with longitudinally oriented, disorganized and irregular structures (**Fig. 4d** and **Supplementary Fig. 4c**).

These results suggest that alteration of the T tubule network is an early and specific event following *Bin1* exon 11 alteration. Notably, isometric strength measurement of the tibialis anterior muscles showed that skipping of *Bin1* exon 11 induced a ~28% decrease ($n = 11$, $P = 0.00034$) in specific muscle strength (**Fig. 4e**). We noted some variability in *Bin1* exon 11 skipping inherent to the AAV exon-skipping strategy[31], which is a milder approach compared to lethal

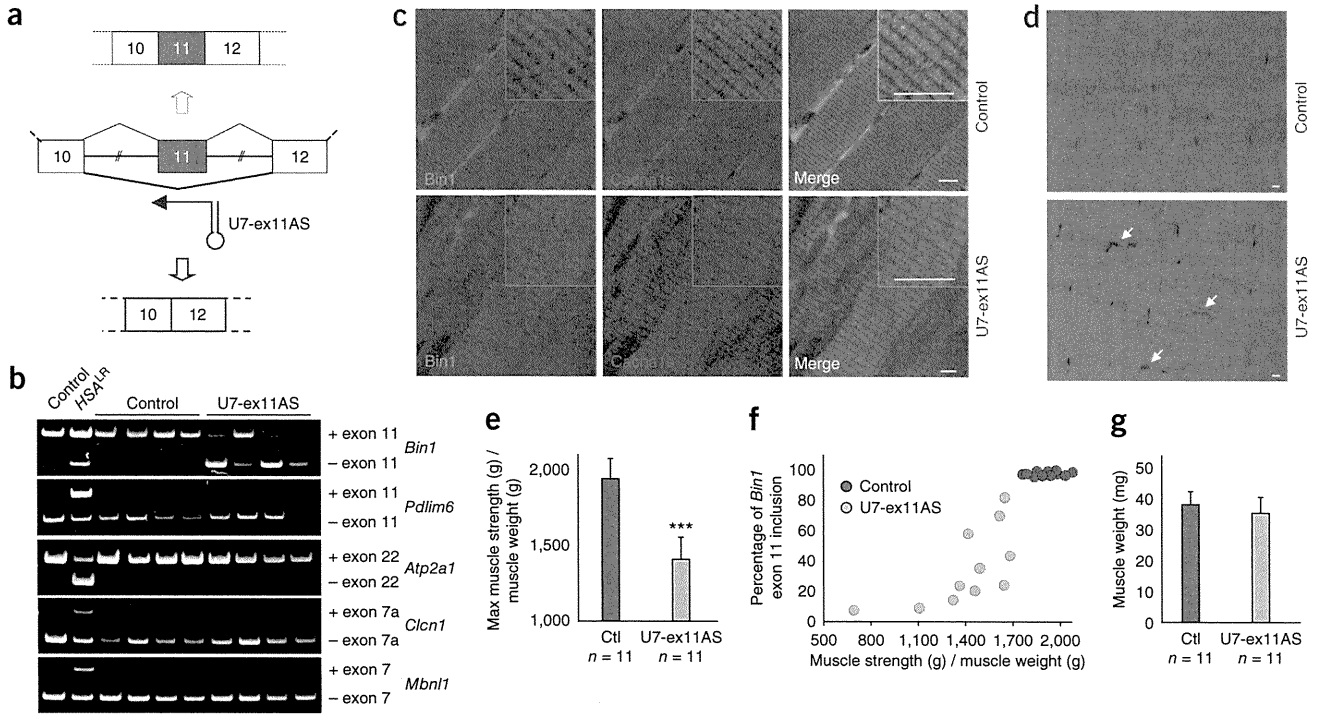

Figure 4 Skipping of *Bin1* exon 11 is sufficient to induce muscle weakness in mice. (**a**) Schematic representation of the U7-exon 11 antisense construct (U7-ex11AS). (**b**) RT-PCR analysis of *Bin1* exon 11, *Pdlim6* (encoding Ldb3, also known as Zasp or cypher) exon 11, *Atp2a1* exon 22, *Clcn1* exon 7a and *Mbnl1* exon 7 from total RNA extracted from tibialis anterior muscles of wild-type mice 4 months after injection of control AAV2/1 or AAV2/1 encoding the U7-ex11AS construct. RNA samples of transgenic mice expressing 250 expanded CUG repeats in skeletal muscle (HSA^{LR} mice)[6] were used as a positive control. (**c**) Confocal microscopy analysis of immunofluorescence labeling of Bin1 and Cacna1s in longitudinal paraffin-embedded sections of TA muscle injected with control AAV2/1 or AAV2/1 encoding the U7-ex11AS construct. Insets, higher magnifications of Bin1 localization. Scale bars, 10 μm. (**d**) Electron microscopy analysis of osmium tetroxide–potassium ferricyanide–stained longitudinal sections of tibialis anterior muscles of wild-type mice 4 months after injection of control AAV2/1 or AAV2/1 encoding the U7-ex11AS construct. White arrows indicate altered T tubule structures. Scale bars, 100 nm. (**e–g**) Measures of the absolute maximal isometric tetanic force (**e**), of the tetanic force relative to the inclusion of *Bin1* exon 11 (**f**) and of the muscle weight (**g**) of isolated TA muscle injected with vehicle alone (PBS, $n = 2$), AAV2/1 expressing a control construct ($n = 9$) or AAV2/1 expressing the U7-ex11AS construct ($n = 11$). As no differences between vehicle alone ($n = 2$) or control AAV2/1 ($n = 9$) were observed, data were pooled and are indicated as generic control ($n = 11$). Data are presented as means ± s.d. $^{***}P < 0.001$.

knockout of *Bin1* (ref. 32). The extent of muscle weakness correlated ($R^2 = 0.62$) with the degree of *Bin1* exon 11 skipping (**Fig. 4f**), suggesting a direct correlation between *Bin1* splicing misregulation and muscle weakness. This is reminiscent of our findings in people with myotonic dystrophy, in whom we observed near-complete BIN1 exon 11 absence in the severe congenital CDM1 form, whereas we saw only partial splicing alteration in the milder adult DM1 and DM2 forms. Although muscle weakness was evident in the mice with exon 11 skipping, we observed no significant muscle mass loss 4 months after injection (**Fig. 4g**), suggesting that T tubule alterations and muscle weakness preceded muscle atrophy or degeneration. In addition, we observed similar Bin1 mislocalization and muscle weakness when we injected muscles of adult wild-type mice (**Supplementary Fig. 4d–f**), suggesting that Bin1 is required both postnatally and in adulthood.

T tubule alterations and muscle weakness have also been reported in a CNM mouse model in which the *Mtm1* gene was deleted[33]. These alterations were accompanied by a decreased expression of Cacna1s, spurring us to determine whether similar changes occurred in our *Bin1* model. Quantitative RT-PCR and western blotting showed a significant ($P < 0.05$) decrease in Cacna1s expression in muscles injected with U7-ex11AS virus compared to control contralateral-injected muscles (**Supplementary Fig. 4g,h**). Overall, these results suggest that misregulation of *Bin1* exon 11 splicing is sufficient to induce alterations of T tubules and of Cacna1s, a key regulator of the excitation-contraction coupling process, ultimately resulting in muscle weakness.

In conclusion, our results suggest a model (**Supplementary Fig. 5**) in which the alternative splicing of the muscle-specific exon 11 of *BIN1* mRNA is regulated by the MBNL1 splicing factor. Sequestration of MBNL1 by expanded CUG or CCUG repeats in individuals with DM1 or DM2, respectively, leads to skipping of that exon and expression of an isoform of BIN1 unable to bind PtdIns5P and tubulate membranes, which ultimately results in disorganized T tubules and altered excitation-contraction coupling. We propose that missplicing of *BIN1* and of other pre-mRNAs involved in excitation-contraction coupling[34] (ryanodine receptor 1 (skeletal) (*RYR1*), *ATP2A1*, *ATP2A2* and so on) ultimately results in muscle weakness in humans with myotonic dystrophy. This model is consistent with previous finding of T tubule alterations[30] and calcium homeostasis alterations[34,35] in muscle cells in humans with, and mouse models of, myotonic dystrophy. Furthermore, we propose that the MTM1 phosphatase produces PtdIns5P-enriched membranes, which are recognized by exon 11 of BIN1, resulting in membrane tubulation (**Supplementary Fig. 5**). This model is consistent with previous reports of T tubule elongation through accretion of cytoplamic vesicles[36], recent observations of BIN1 and T tubule alterations in humans with, and animal models of, CNM[33,37,38] and case reports of congenital myopathies with central nuclei resulting from mutations in *RYR1* (ref. 39). These data suggest that a common

mechanism, involving T tubule biogenesis by BIN1 leading to alterations of the calcium homeostasis coupled to the excitation-contraction process, may underlie muscle weakness in myotonic dystrophy and centronuclear myopathy.

METHODS

Methods and any associated references are available in the online version of the paper at http://www.nature.com/naturemedicine/.

Accession codes. Microarray data have been deposited in the Gene Expression Omnibus (GEO) with accession code GSE21795.

Note: Supplementary information is available on the Nature Medicine website.

ACKNOWLEDGMENTS

We thank T. Cooper (Baylor College of Medicine) for the gift of the β-globin 4.11.12, DMPKS, DT960 and tgCUGBP1 plasmids, L. Ranum (University of Minnesota) for the gift of the CCTG300 expression plasmid, C. Branlant (CNRS) for the gift of the pGEX-MBNL1Δ101 vector, M. Swanson (University of Florida) for the gift of the pGEX-6P-MBNL1-His vector, P. Hawkins (Babraham Research Campus) for the gift of the GFP-PH domain of PLCg and GFP-PX domain of P40 constructs, O. Gozani (Stanford University) for the gift of the GFP-PHD domain of ING2 vector, Z. Xue (Université Paris 7) for the gift of the synemin-specific antibody, I. Marty (INSERM) for the gift of the RYR1-specific antibody, M. Swanson (University of Florida), G. Gourdon (INSERM) and C. Thornton (University of Rochester) for the gift of RNA from skeletal muscles of MBNL1$^{\Delta E3}$, DM300 and HSA^{LR} mice, respectively, the IGBMC facilities for assistance, J. Lainé, G. Butler-Browne and all members of the French DM Network for fruitful discussion. This work was supported by INSERM AVENIR (N.C.-B.), Agence nationale de la recherche GENOPAT 07-942 (N.C.-B.), 08-005 (J.L.) and BLANC 07-065 (J.L.), Association Française contre les Myopathies MNM1 12982 (N.C.-B.), 12570 and 14269 (D.F.), 12576 and 14058 (J.L.), Fondation pour la Recherche Médicale 20071210538 (J.L.), Japan Society for the Promotion of Science KAKENHI 20590998 (M.P.T.) and a European Molecular Biology Organization long-term fellowship (Y.I.).

AUTHOR CONTRIBUTIONS

Experiments were carried out by C.F., A.F.K., C.H., S.V., Y.I., A.T., V.T., A.V., A.F., N.M., Y.K., R.T., V.F., G.P., C.B.-L. F.D. and M.-C.H. Bioinformatic analyses were done by P.d.l.G., D.D., C.T. and D.A. Clinical samples and patient data were from A.L.d.M., N.S., A.L., B.U., B.S., M.P.T., I.N., G.B. and D.F. Data were collected and analyzed by N.M., C.T., D.A., L.G., P.Z., I.N., M.P.T., B.U., B.S., G.B., J.L., D.F. and N.C.-B. The study was designed, coordinated and written by D.F. and N.C.-B.

COMPETING FINANCIAL INTERESTS

The authors declare no competing financial interests.

Published online at http://www.nature.com/naturemedicine/.
Reprints and permissions information is available online at http://www.nature.com/reprints/index.html.

1. Brook, J.D. *et al.* Molecular basis of myotonic dystrophy: expansion of a trinucleotide (CTG) repeat at the 3′ end of a transcript encoding a protein kinase family member. *Cell* **68**, 799–808 (1992).
2. Fu, Y.H. *et al.* An unstable triplet repeat in a gene related to myotonic muscular dystrophy. *Science* **255**, 1256–1258 (1992).
3. Mahadevan, M. *et al.* Myotonic dystrophy mutation: an unstable CTG repeat in the 3′ untranslated region of the gene. *Science* **255**, 1253–1255 (1992).
4. Liquori, C.L. *et al.* Myotonic dystrophy type 2 caused by a CCTG expansion in intron 1 of ZNF9. *Science* **293**, 864–867 (2001).
5. Philips, A.V., Timchenko, L.T. & Cooper, T.A. Disruption of splicing regulated by a CUG-binding protein in myotonic dystrophy. *Science* **280**, 737–741 (1998).
6. Mankodi, A. *et al.* Myotonic dystrophy in transgenic mice expressing an expanded CUG repeat. *Science* **289**, 1769–1773 (2000).
7. Seznec, H. *et al.* Mice transgenic for the human myotonic dystrophy region with expanded CTG repeats display muscular and brain abnormalities. *Hum. Mol. Genet.* **10**, 2717–2726 (2001).
8. Miller, J.W. *et al.* Recruitment of human muscleblind proteins to (CUG)*n* expansions associated with myotonic dystrophy. *EMBO J.* **19**, 4439–4448 (2000).
9. Kanadia, R.N. *et al.* A muscleblind knockout model for myotonic dystrophy. *Science* **302**, 1978–1980 (2003).
10. Ho, T.H. *et al.* Muscleblind proteins regulate alternative splicing. *EMBO J.* **23**, 3103–3112 (2004).
11. Kuyumcu-Martinez, N.M., Wang, G.S. & Cooper, T.A. Increased steady-state levels of CUGBP1 in myotonic dystrophy 1 are due to PKC-mediated hyperphosphorylation. *Mol. Cell* **28**, 68–78 (2007).
12. Savkur, R.S., Philips, A.V. & Cooper, T.A. Aberrant regulation of insulin receptor alternative splicing is associated with insulin resistance in myotonic dystrophy. *Nat. Genet.* **29**, 40–47 (2001).
13. Mankodi, A. *et al.* Expanded CUG repeats trigger aberrant splicing of ClC-1 chloride channel pre-mRNA and hyperexcitability of skeletal muscle in myotonic dystrophy. *Mol. Cell* **10**, 35–44 (2002).
14. Charlet-Berguerand, N. *et al.* Loss of the muscle-specific chloride channel in type 1 myotonic dystrophy due to misregulated alternative splicing. *Mol. Cell* **10**, 45–53 (2002).
15. Jungbluth, H., Wallgren-Pettersson, C. & Laporte, J. Centronuclear (myotubular) myopathy. *Orphanet J. Rare Dis.* **3**, 26 (2008).
16. Laporte, J. *et al.* A gene mutated in X-linked myotubular myopathy defines a new putative tyrosine phosphatase family conserved in yeast. *Nat. Genet.* **13**, 175–182 (1996).
17. Bitoun, M. *et al.* Mutations in dynamin 2 cause dominant centronuclear myopathy. *Nat. Genet.* **37**, 1207–1209 (2005).
18. Nicot, A.S. *et al.* Mutations in amphiphysin 2 (BIN1) disrupt interaction with dynamin 2 and cause autosomal recessive centronuclear myopathy. *Nat. Genet.* **39**, 1134–1139 (2007).
19. Lee, E. *et al.* Amphiphysin 2 (BIN1) and T tubule biogenesis in muscle. *Science* **297**, 1193–1196 (2002).
20. Peter, B.J. *et al.* BAR domains as sensors of membrane curvature: the amphiphysin BAR structure. *Science* **303**, 495–499 (2004).
21. Razzaq, A. *et al.* Amphiphysin is necessary for organization of the excitation-contraction coupling machinery of muscles, but not for synaptic vesicle endocytosis in *Drosophila*. *Genes Dev.* **15**, 2967–2979 (2001).
22. Dansithong, W. *et al.* MBNL1 is the primary determinant of focus formation and aberrant insulin receptor splicing in DM1. *J. Biol. Chem.* **280**, 5773–5780 (2005).
23. Hino, S. *et al.* Molecular mechanisms responsible for aberrant splicing of SERCA1 in myotonic dystrophy type 1. *Hum. Mol. Genet.* **16**, 2834–2843 (2007).
24. Yuan, Y. *et al.* Muscleblind-like 1 interacts with RNA hairpins in splicing target and pathogenic RNAs. *Nucleic Acids Res.* **35**, 5474–5486 (2007).
25. Kino, Y. *et al.* MBNL and CELF proteins regulate alternative splicing of the skeletal muscle chloride channel CLCN1. *Nucleic Acids Res.* **37**, 6477–6490 (2009).
26. Kalsotra, A. *et al.* A postnatal switch of CELF and MBNL proteins reprograms alternative splicing in the developing heart. *Proc. Natl. Acad. Sci. USA* **105**, 20333–20338 (2008).
27. Kanadia, R.N. *et al.* Reversal of RNA missplicing and myotonia after muscleblind overexpression in a mouse poly(CUG) model for myotonic dystrophy. *Proc. Natl. Acad. Sci. USA* **103**, 11748–11753 (2006).
28. Teplova, M. & Patel, D.J. Structural insights into RNA recognition by the alternative-splicing regulator muscleblind-like MBNL1. *Nat. Struct. Mol. Biol.* **15**, 1343–1351 (2008).
29. Tronchère, H. *et al.* Production of phosphatidylinositol 5-phosphate by the phosphoinositide 3-phosphatase myotubularin in mammalian cells. *J. Biol. Chem.* **279**, 7304–7312 (2004).
30. Ueda, H. *et al.* Decreased expression of myotonic dystrophy protein kinase and disorganization of sarcoplasmic reticulum in skeletal muscle of myotonic dystrophy. *J. Neurol. Sci.* **162**, 38–50 (1999).
31. Goyenvalle, A. *et al.* Rescue of dystrophic muscle through U7 snRNA-mediated exon skipping. *Science* **306**, 1796–1799 (2004).
32. Muller, A.J. *et al.* Targeted disruption of the murine Bin1/amphiphysin II gene does not disable endocytosis but results in embryonic cardiomyopathy with aberrant myofibril formation. *Mol. Cell. Biol.* **23**, 4295–4306 (2003).
33. Al-Qusairi, L. *et al.* T tubule disorganization and defective excitation-contraction coupling in muscle fibers lacking myotubularin lipid phosphatase. *Proc. Natl. Acad. Sci. USA* **106**, 18763–18768 (2009).
34. Kimura, T. *et al.* Altered mRNA splicing of the skeletal muscle ryanodine receptor and sarcoplasmic/endoplasmic reticulum Ca^{2+}-ATPase in myotonic dystrophy type 1. *Hum. Mol. Genet.* **14**, 2189–2200 (2005).
35. Osborne, R.J. *et al.* Transcriptional and post-transcriptional impact of toxic RNA in myotonic dystrophy. *Hum. Mol. Genet.* **18**, 1471–1481 (2009).
36. Yuan, S. *et al.* Biogenesis of transverse tubules: immunocytochemical localization of a transverse tubular protein (TS28) and a sarcolemmal protein (SL50) in rabbit skeletal muscle developing in situ. *J. Cell Biol.* **110**, 1187–1198 (1990).
37. Dowling, J.J. *et al.* Loss of myotubularin function results in T tubule disorganization in zebrafish and human myotubular myopathy. *PLoS Genet.* **5**, e1000372 (2009).
38. Toussaint, A. *et al.* Defects in amphiphysin 2 (BIN1) and triads in several forms of centronuclear myopathies. *Acta Neuropathol.* **121**, 253–266 (2010).
39. Wilmshurst, J.M. *et al.* RYR1 mutations are a common cause of congenital myopathies with central nuclei. *Ann. Neurol.* **68**, 717–726 (2010).

ONLINE METHODS

RT-PCR analysis of *BIN1*. In accordance with the Helsinki Declaration, all human samples were collected after informed consent and with the appropriate oversight of the ethical committees of the following institutions: the Department of Neurology of the University of Osaka, the Center of Neurology and Psychiatry of Tokyo, the Centro de Investigación Biomédica en Red Sobre Enfermedades Neurodegenerativas, the Jean Pierre Aubert Research Center, the Department of Pathology of the University of Rouen, the Department of Neuromuscular Research of the University of Tampere, the Friedrich Baur Institute of the University Ludwig Maximilian and the Institut Mondor de Recherche Biomédicale. Total RNA isolated from homogenized skeletal muscle was subjected to RT–PCR analysis using primers that anneal within human *BIN1* exon 10 (forward: 5′-AGAACCTCAATGATGTGCTGG-3′) and *BIN1* exon 12 (reverse: 5′-TCGTGGTTGACTCTGATCTCGG-3′), resulting in PCR products of 208 bp (+ exon 11) and 163 bp (− exon 11). For mouse, the primers anneal within *Bin1* exon 10 (forward: 5′-TCAATGATGTCCTGGTCAGC-3′) and exon 12 (reverse: 5′-GCTCATGGTTCACTCTGATC-3′), PCR products are of 207 (+ exon 11) and 162 (− exon 11) bp.

BIN1 minigene construction and analysis. We PCR-amplified 229 nucleotides of upstream intron 10, BIN1 exon 11 and 220 nucleotides of downstream intron 11 (NT_022135.16) from human DNA (Clontech) and inserted the product between the HincII and BamHI restriction sites of the β-globin 4.11.12 vector (gift from T. Cooper). Next, the last 325 base pairs of intron 11 followed by BIN1 exon 12 were similarly amplified and inserted between the BamHI and NcoI restriction sites to replace the last β-globin exon. Mutations in BIN1 intron 11 were introduced by primer-directed PCR mutagenesis. C2C12 cells plated in six-well plates were co-transfected with Lipofectamine 2000 (Invitrogen) according to the manufacturer's instructions with *BIN1* minigene and DMPKS, DT960, GFP-CUGBP1 (NM_006560), GFP-MBNL1 40 kDa (NM_207292), siRNA (Eurogentec) directed against MBNL1 (5′-AACACGGAAUGUAAAU UUGCADTDT-3′) or against CUGBP1 (5′-GUUACGACAAUCCUGUUUCD TDT-3′) in DMEM medium containing 1 g l^{-1} glucose and 2% horse serum (37 °C, 5% CO_2) over 24 h. Total RNAs were extracted with Tri Reagent (Molecular Research Center) and subjected to reverse transcription by the Transcriptor Reverse Transcriptase kit (Roche). PCR was performed with Taq polymerase (Roche), one denturation step at 94 °C for 2 min, 25 cycles of amplification 94 °C for 1 min, 58 °C for 45 s, 72 °C for 1 min and a final step at 72 °C for 7 min using the forward primer 5′-CATTCACCACATTGGTGT GC-3′ and the reverse primer 5′-AAGTGATCCTAGACTAGCCGCC-3′ specific to the β-globin–*BIN1* minigene. The PCR products of mRNAs including and excluding exon 11 are of 345 and 300 bp, respectively. PCR products were precipitated, analyzed by eletrophoresis on a 6.5% polyacrylamide gel, stained with ethidium bromide and quantified with a Typhoon scanner.

Fluorescent *in situ* hybridization and immunofluorescence. The combined FISH–immunofluorescence experiment was done as described previously[22] with a Cy3-conjugated PNA (CAG)7x probe, a monoclonal mouse antibody to BIN1 (clone 99D directed against exon 17, Upstate, 1 in 200 dilution) and a secondary Alexa 488–conjugated goat antibody to mouse IgG (Invitrogen) or Cy3-conjugated donkey antibody to mouse IgG (Jackson ImmunoResearch). Other antibodies used were a monoclonal antibody to CACNA1S (DHPRα1 or CAV1.1) (mAB-1a, Chemicon, 1 in 100 dilution), polyclonal antibody to synemin (desmuslin) (gift from Z. Xue, 1 in 400), polyclonal antibody to desmin (Chemicon, 1 in 100), monoclonal antibody to ATP2A1 (clone IIH11, Abcam, 1 in 100), monoclonal antibody to RYR1 (clone 34C, Sigma, 1 in 100), monoclonal antibody to ACTN1 (clone SA20, Abnova) and polyclonal rabbit antibody to BIN1 (H100, SantaCruz, 1 in 100). Images were captured with a Leica confocal microscope and software (Leica Microsytems) and processed with Adobe Photoshop software.

***In vivo* gene transfer.** All mouse procedures were done according to protocol approved by the Committee on Animal Resources at the Centre d'Exploration Fonctionnelle of Pitie-Salpetriere animal facility and under appropriate biological containment. The U7-ex11AS construct and AAV production were done as previously described[28]. The tibialis anterior muscles of five male and six female newborns (10 d old) or adult female (2 months old) C57BL/6 mice were injected with respectively 10 or 50 µl of physiological solution containing the AAV2/1 vectors (1.8×10^{13} vector genomes per ml). For each mouse, one tibialis anterior muscle was injected with AAV (U7-ex11AS), and the contralateral muscle was injected with control AAV containing any transgene or vehicle alone (PBS). Four months after injections, mice were killed, muscles were collected and snap-frozen in liquid nitrogen–cooled isopentane and stored at −80 °C.

***In situ* force measurement.** The isometric contractile properties of tibialis anterior muscles (TA) were studied *in situ* as previously described[40] (Mouisel, E. *et al.*, 2006). Mice were anesthetized with pentobarbital (60 mg per kg body weight). The knee and foot were fixed with clamps and pins. The distal tendon of the tibialis anterior muscle was attached to a lever arm of a servomoteur system (305B, Dual-Mode Lever). Data were recorded and analyzed on a microcomputer using PowerLab system (4SP, ADInstruments) and software (Chart 4, ADInstruments). The sciatic nerve (proximally crushed) was stimulated by a bipolar silver electrode using a supramaximal (10-V) square wave pulse of 0.1 ms duration. Absolute maximal isometric tetanic force was measured during isometric contractions in response to electrical stimulation (frequency of 25 to 150 Hz, train of stimulation of 500 ms). Specific P0 was calculated by dividing P0 by muscle weight.

Additional methods. Detailed methodology is described in the **Supplementary Methods**.

40. Mouisel, E. *et al.* Outcome of acetylcholinesterase deficiency for neuromuscular functioning. *Neurosci. Res.* **55**, 389–396 (2006).

doi:10.1038/nm.2374

Int. J. Mol. Sci. **2011**, *12*, 1660-1671; doi:10.3390/ijms12031660

OPEN ACCESS

International Journal of
Molecular Sciences
ISSN 1422-0067
www.mdpi.com/journal/ijms

Review

The Role of Alpha-Dystrobrevin in Striated Muscle

Masayuki Nakamori [1,2] and Masanori P. Takahashi [1,*]

[1] Department of Neurology, Osaka University Graduate School of Medicine, 2-2, D-4, Yamadaoka, Suita, Osaka 565-0871, Japan; E-Mail: masayuki_nakamori@urmc.rochester.edu

[2] Department of Neurology, University of Rochester Medical Center, 601 Elmwood Avenue, Box 645 URMC, Rochester, NY 14642, USA

* Author to whom correspondence should be addressed;
E-Mail: mtakahas@neurol.med.osaka-u.ac.jp; Tel.: +81-6-6879-3571; Fax: +81-6-6879-3579.

Received: 16 December 2010; in revised form: 29 January 2011 / Accepted: 23 February 2011 / Published: 4 March 2011

Abstract: Muscular dystrophies are a group of diseases that primarily affect striated muscle and are characterized by the progressive loss of muscle strength and integrity. Major forms of muscular dystrophies are caused by the abnormalities of the dystrophin glycoprotein complex (DGC) that plays crucial roles as a structural unit and scaffolds for signaling molecules at the sarcolemma. α-Dystrobrevin is a component of the DGC and directly associates with dystrophin. α-Dystrobrevin also binds to intermediate filaments as well as syntrophin, a modular adaptor protein thought to be involved in signaling. Although no muscular dystrophy has been associated within mutations of the α-dystrobrevin gene, emerging findings suggest potential significance of α-dystrobrevin in striated muscle. This review addresses the functional role of α-dystrobrevin in muscle as well as its possible implication for muscular dystrophy.

Keywords: dystrobrevin; syntrophin; dystrophin; DGC; muscular dystrophy; signaling; intermediate filament; splicing

1. Introduction

α-Dystrobrevin is a member of the dystrophin gene family with homology to the cysteine-rich carboxy-terminal domain of dystrophin [1,2]. α-Dystrobrevin was identified as human and mouse homologues of an 87 kDa phosphoprotein found at the Torpedo electric organ post-synaptic

membrane [1,3,4]. In striated muscle, dystrobrevin and dystrophin are both localized to the cytoplasmic face of the sarcolemma, and form a macromolecular complex with a variety of proteins and glycoproteins, termed dystrophin-glycoprotein complex (DGC) [5]. The DGC plays crucial roles in maintaining the structural integrity of muscle fibers by linking the extracellular matrix to the subsarcolemmal cytoskeleton, and also provides a scaffold for signaling molecules. The abnormalities of the DGC are recognized to be responsible for several forms of progressive muscular dystrophies. The absence of dystrophin results in loss of the entire DGC from the sarcolemma and leads to Duchenne muscular dystrophy (DMD) [6]. Mutations in sarcoglycan genes, one of the components of the DGC, result in several types of limb-girdle muscular dystrophy (sarcoglycan-deficient LGMD or SD-LGMD). Although α-dystrobrevin directly associates with dystrophin and sarcoglycan complex [7,8], no mutation has been identified in muscular dystrophy patients hitherto. However, α-dystrobrevin knockout mice, which demonstrate mild myopathy, have provided clues of its potential functions in striated muscle [9]. Recently, α-dystrobrevin is known to be subject to extensive alternative splicing [4,10], which results in changes in its subcellular distribution and function in muscle [11]. Furthermore, a number of binding partner of dystrobrevin have been identified. In this review, we focus on the recent findings regarding the alternative splicing of α-dystrobrevin, its interactions with other proteins, and implications for muscular dystrophy.

2. α-Dystrobrevin Gene and Transcripts

The mammalian dystrobrevin protein family is comprised of α- and β-dystrobrevin which are encoded by the *DTNA* and *DTNB* gene, respectively [4,12]. α-Dystrobrevin is expressed predominantly in muscle and brain whereas β-dystrobrevin is expressed in non-muscle tissues [3,4,12]. The human α-dystrobrevin gene consists of 23 coding exons [10].

α-Dystrobrevin is known to be subject to extensive splicing regulation. The alternative usage of three exons—21, 17B, and 11B—generates transcripts of different lengths encoding three major α-dystrobrevin isoforms in human skeletal muscle: α-dystrobrevin 1, α-dystrobrevin 2, and α-dystrobrevin 3 [10] (Figure 1). Additional diversity is observed due to alternative splicing within the coding regions referred to as variable regions 1, 2 and 3 [4]. Firstly, variable region 1 (vr1) consists of a short exon encoding three amino acids (exon 9). In mouse, the transcripts including this exon are primarily restricted to brain [4,13], but are present in brain, heart, and skeletal muscle in human [10]. Variable region 2 (vr2) consists of exons 17A and 17B. Exon 17B encodes the unique *C*-terminal tail of α-dystrobrevin 2. The first 21 nucleotides of exon 17B are also found in the α-dystrobrevin 1 transcript as a result of splicing at a cryptic site [14]. In mouse, the expression of the vr2 region in the α-dystrobrevin 1 transcript appears to be developmentally regulated [13]. Lastly, variable region 3 (vr3) consists of exons 11A, 11B and 12. Exon 11B encodes the unique *C*-terminal tail of α-dystrobrevin 3. In α-dystrobrevin 1 and α-dystrobrevin 2, four in-frame alternatively spliced transcripts, may arise by joining exon 10 with either exon 11A, 12 or 13, or by joining exon 11A with either 12 or 13 (*i.e.*, 10-11A-13, 10-12-13, 10-13, 10-11A-12-13) [10]. In mouse skeletal muscle, the splicing of vr3 has also been reported to be developmentally controlled [13,15,16]. Previous analyses of mouse myoblast cultures demonstrated a transition from α-dystrobrevin lacking vr3 (Δvr3) to α-dystrobrevin including vr3 (+vr3) during differentiation. We also showed that the frequency of vr3